

1 **Induction and dorsal restriction of *Paired-box 3 (Pax3)* gene expression**
2 **in the caudal neuroectoderm is mediated by integration of multiple**
3 **pathways on a short neural crest enhancer**

4
5 **Oraly Sanchez-Ferras, Guillaume Bernas, Emilie Laberge-Perrault and Nicolas Pilon.**

6
7 Molecular Genetics of Development Laboratory, Department of Biological Sciences and BioMed
8 Research Center, Faculty of Sciences, University of Quebec at Montreal (UQAM)

9
10 **Running title:** Regulation of *Pax3* neural expression by a Cdx-Zic2 complex

11
12 **To whom correspondence should be addressed:** Nicolas Pilon, Department of Biological Sciences
13 and BioMed Research Center, Faculty of Sciences, University of Quebec at Montreal (UQAM), 141
14 President-Kennedy Ave, Montreal, PQ, Canada, H2X 3Y7; Tel.: 514-987-3000 x3342; Fax: 514-987-
15 4647; Email: pilon.nicolas@uqam.ca

16
17
18 **ABSTRACT:**

19 *Pax3* encodes a paired-box transcription factor with key roles in neural crest and neural tube
20 ontogenesis. Robust control of *Pax3* neural expression is ensured by two redundant sets of cis-
21 regulatory modules (CRMs) that integrate anterior-posterior (such as Wnt- β Catenin signaling) as well
22 as dorsal-ventral (such as Shh-Gli signaling) instructive cues. In previous work, we sought to
23 characterize the Wnt-mediated regulation of *Pax3* expression and identified the Cdx transcription
24 factors (Cdx1/2/4) as critical intermediates in this process. We identified the neural crest enhancer-2
25 (NCE2) from the 5'-flanking region of *Pax3* as a Cdx-dependent CRM that recapitulates the restricted
26 expression of *Pax3* in the mouse caudal neuroectoderm. While this is consistent with a key role in
27 relaying the inductive signal from posteriorizing Wnt ligands, the broad expression of Cdx proteins in
28 the tailbud region is not consistent with the restricted activity of NCE2. This implies that other positive
29 and/or negative inputs are required and, here, we report a novel role for the transcription factor Zic2 in
30 this regulation. Our data strongly suggests that Zic2 is involved in the induction (as a direct *Pax3*NCE2
31 activator and Cdx neural cofactor) as well as the maintenance of *Pax3* dorsal restriction (as a target of
32 the ventral Shh repressive input). We also provide evidence that the inductive Cdx-Zic2 interaction is
33 integrated on NCE2 with a positive input from the neural-specific transcription factor Sox2. Altogether,
34 our data provide important mechanistic insights into the coordinated integration of different signaling
35 pathways on a short *Pax3* CRM.

36
37
38 **KEY WORDS:** Cdx, Zic, Sox2, Pax3, neural crest cells, neural tube.

42 **1-INTRODUCTION**

43 Building an embryo from an initial population of equivalent cells requires precise spatiotemporal
44 control of gene expression. Information to do this comes from just a few numbers of conserved
45 signaling pathways, is transmitted by DNA binding proteins and interpreted at the cis-regulatory level
46 on evolutionarily conserved genomic sequences. Redundant and different operating enhancers may
47 exist to refine and protect expression of developmental genes from fluctuations in these signals or
48 mutations in the genome. Subsequently, the output of gene expression and gene regulatory interactions
49 provide the memory to maintain established expression patterns in the absence of signaling inputs. In
50 this regard, a lot of work has been done to understand the molecular mechanisms of neural gene
51 expression during establishment of the anterior-posterior (AP) as well as the dorsal-ventral (DV) axes.
52 Nevertheless, how both AP and DV signaling inputs are coordinately integrated at the cis-regulatory
53 level is still poorly understood.

54
55 *Pax3/7* (Paired box 3 and 7) and *Zic* (Zinc finger protein of the cerebellum) family members (*Zic1-5*)
56 encode transcription factors that exhibit overlapping expression domains in the neuroectoderm along
57 both the AP and the DV axis. During neurulation, expression of these genes is similarly restricted to
58 pre-migratory neural crest cells (NCC) and dorsal neural tube (NT) [1-9]. However, such overlap is less
59 extensive along the AP axis and most especially in the caudal embryo where only *Pax3* and the
60 *Zic2/Zic5* gene pair are expressed in the posterior neural plate (PNP) [1, 10]. Consistent with their wide
61 expression pattern and key developmental role, loss-of-function mutations of *Pax3* and *Zic2* – as seen
62 for example in the *Splotch* (*Pax3*) and *Kumba* (*Zic2*) mouse mutants – causes severe and similar NT
63 and NCC defects affecting the entire AP axis such as spina bifida, craniofacial malformations, absence
64 of dorsal root ganglia and pigmentary anomalies [6, 7, 10-12].

65
66 Work performed in several vertebrate species has revealed that AP instructive cues from Wnt
67 (Wingless and Int-1 related) and FGF (fibroblast growth factor) pathways as well as DV instructive
68 cues from BMP (bone morphogenetic protein) and Shh (Sonic Hedgehog) pathways are all involved in
69 the induction and dorsal restriction of *Pax3/7* and *Zic* members [8, 13-22]. These studies notably point
70 to a critical role for posteriorizing canonical Wnt signaling and intermediate levels of BMP molecules
71 during induction in the neural plate [14, 16-18, 23, 24] whereas opposing gradients of dorsal BMP and
72 ventral Shh signaling are subsequently implicated in the maintenance and dorsal restriction in the
73 closed NT [19-21, 25]. Although the general role of these pathways is well accepted, some species-
74 specific variations are also expected regarding their relative importance. In the case of *Pax3*, this is
75 well exemplified by the comparison of its posterior expression domain between chick and mouse
76 embryos. Indeed, in chick embryos, *Pax3* expression is initially induced in the whole PNP before
77 becoming restricted to the dorsal NT whereas in mouse embryos, *Pax3* expression is already restricted
78 to the lateral borders of the PNP during the induction phase [15, 26].

79
80 Multiple evolutionary conserved cis-regulatory modules (CRMs) have been identified for *Pax3*. These
81 CRMs are clustered in two areas of the *Pax3* locus: one in the 5'-flanking region and the other in
82 intron-4 [27-29]. The 5'-flanking region, named Neural Crest Enhancer (NCE), is located within the

83 1.6 Kb proximal promoter and is subdivided in two short CRMs of approximately 250 bp named NCE1
 84 and NCE2 [27, 28]. The entire NCE is not only able to direct *Pax3* reporter expression in mouse NCC
 85 and dorsal NT along the hindbrain and trunk region, but also drive enough functional expression levels
 86 of *Pax3* to rescue the NT and NCC defects observed in *Pax3* Splotch mice [7]. Interestingly, targeted
 87 deletion studies in the mouse have suggested that NCE acts redundantly with a second evolutionary
 88 conserved region (ECR2) located in the 4th intron [29]. In fact, more recent work using the zebrafish as
 89 a model has demonstrated that the *Pax3* intron-4 contains at least two CRMs that appears to exhibit
 90 complementary activities in order to recapitulate the induction, dorsal restriction and maintenance of
 91 *Pax3* neural expression [18, 30]. Given that the effect of their deletion has not been documented so far,
 92 the requirement of any of these intron-4 CRMs for *Pax3* expression as well as their relative importance
 93 over the 5'-flanking NCE is currently unknown.

94
 95 We have previously demonstrated that the NCE2 region alone is able to recapitulate both the induction
 96 and dorsal restriction of *Pax3* expression in the caudal NCC and NT [26], suggesting that this CRM is
 97 well suited for analyzing the coordinated integration of both AP and DV instructive cues. In this regard,
 98 we have already demonstrated that activity of this enhancer depends on a positive input from caudal-
 99 related homeobox (Cdx) transcription factors downstream of Wnt/ β Catenin signaling [26]. Here we
 100 further show that, in addition to Cdx, Zic2 also directly regulates murine *Pax3* expression and acts as a
 101 Cdx neural cofactor. Importantly; we show that the NCE2 region integrates positive inputs from caudal
 102 Cdx, dorsal Zic2 as well as neural Sox2 transcription factors. Furthermore, we provide evidence for a
 103 putative role of Zic2/5 as mediators of the Shh-induced repressive input involved in the dorsal
 104 restriction of *Pax3* expression. Taken together with previous descriptions of other functional binding
 105 sites (e.g. Brn1 and Tead2) within NCE2 [28, 31], our data strongly suggest that this short CRM
 106 behaves as a “super-enhancer” [32] that mediates the spatiotemporal induction and dorsal restriction of
 107 *Pax3* expression in the mouse caudal neuroectoderm.

108 109 **2-MATERIALS and METHODS**

110 111 **2.1-Ethics Statement**

112 Experiments involving mice were performed following Canadian Council of Animal Care (CCAC)
 113 guidelines for the care and manipulation of animals used in medical research. Protocols involving the
 114 manipulation of animals were approved by the institutional ethics committee of the University of
 115 Quebec at Montreal (comité institutionnel de protection des animaux (CIPA)); Reference number 0513-
 116 C1-648-0514).

117 118 **2.2-Plasmid constructs and site-directed mutagenesis**

119 The *Pax3* cDNA vector pBH3.2 [1] was kindly provided by J. Epstein. Expression vectors for FLAG-
 120 tagged Cdx1 and GST-Cdx1 fusion proteins have been described previously [33]. Expression vectors
 121 for FLAG-tagged full-length and deletion mutant ZIC2 proteins were a generous gift from S. Tejpar
 122 [34]. HA-tagged Zic2 expression vector (pcDNA3-HAZic2) was kindly provided by J. Aruga [35]. Myc-
 123 tagged Sox2 expression vector (pcDNA3.1-MycSox2) was a gift from M. Bani-Yaghoub [36]. FLAGCdx1
 124 and HAZic2 expression vectors co-expressing GFP were generated by subcloning the respective cDNA

125 into the pIRES2-EGFP vector (Clontech). Wild type (wt) or CdxBS mutant versions of a *Pax3*NCE2-
 126 luciferase reporter constructs were as previously described [26]. For generating Zic binding site (BS)
 127 mutant versions, point mutations were introduced into the ZicBS of NCE2 by using the Quick Change
 128 Multisite-directed mutagenesis kit (Stratagene) in accordance with manufacturer's instructions.
 129 Sequence of the oligonucleotide used for site-directed mutagenesis of the ZicBS was: 5'-
 130 CGTCATATCCTGCTaaGGACACTTCAGCTCCTAGCCAAGA-3' (with ZicBS underlined and point
 131 mutations indicated by lower case letters).

132

133 ***2.3-In situ hybridization and immunofluorescence analyses***

134 FVB mouse embryos were obtained from timed pregnancies, noon of the day on which a vaginal plug
 135 was detected being considered as embryonic day (e)0.5. Embryos to be compared were stage-matched
 136 in accordance with established criteria [37] and processed in parallel.

137 Whole-mount *in situ* hybridization of *Pax3* and *Zic2* mRNAs was performed using standard approach
 138 [38]. The *Pax3* probe was generated from the pBH3.2 plasmid while the *Zic2* probe was generated
 139 from the pcDNA3-HAZic2 plasmid. Transverse sections (100µm) were prepared using a vibrating blade
 140 microtome Microm HM 650V (Thermo Scientific) as previously described [39]. Images were acquired
 141 with a Leica DFC 495 camera mounted on a Leica M205 FA microscope (Leica Microsystems).

142 Whole mount immunostaining of Nkx6.1 in e9.5 mouse embryos was performed using the protocol
 143 described by [39] and consecutive vibratome transverse sections of the tail were prepared as described
 144 above. Immunofluorescence analyses on NT cryosections were performed as previously described
 145 [40]. Briefly, 20 µm frozen sections were prepared using a Leica CM1950 cryostat (Leica
 146 microsystems) and adjacent sections were used to compare the distribution of Cdx2 and Pax3 proteins.
 147 Sections were blocked with 10% fetal bovine serum, 0.1% TritonX-100 in PBS for 1 hour and then
 148 incubated at 4°C overnight with primary antibodies diluted in blocking solution. Nuclei were stained
 149 using DAPI (Molecular Probes) and slides were then incubated 1 hour at room temperature with
 150 secondary antibodies diluted in blocking solution. Antibodies and dilutions used were: mouse anti-
 151 Cdx2 1: 100 (Biogenex), mouse anti-Pax3 1:400 (R&D Systems), mouse IgG1 anti-NKX6.1 1:20
 152 (Developmental Studies Hybridoma Bank) and Alexa-647 donkey anti-mouse 1:500 (Jackson
 153 Immunoresearch). Images were taken with a Nikon A1 laser-scanning confocal microscope.

154

155 ***2.4-Chromatin immunoprecipitation (ChIP) assays***

156 ChIP assays in Neuro2a (N2a) cells were performed using the M-Fast Chromatin immunoprecipitation
 157 kit (ZmTech Scientific) in accordance with manufacturer's instructions. For immunoprecipitation of
 158 chromatin from _{HA}Zic2- or _{FLAG}Cdx1-transfected N2a cells (10⁶ cells), 1µg of rabbit anti-HA (Abcam)
 159 and mouse anti-FLAG M2 (Sigma) antibodies were respectively used. A normal rabbit IgG serum was
 160 used as a negative control of immunoprecipitation. PCR amplifications were performed using the
 161 Platinum Taq DNA polymerase (Life Technologies) and consisted of 35 cycles of 30s at 96°C, 30s at
 162 60°C and 30s at 72°C. The primers used for this study were: *Pax3* NCE2 Forward (5'-
 163 GGCACAATGGTACCTTCTCTAAGG-3') and Reverse (5'-
 164 CCCTTCTGAGAAGCGGGGACTTTAAA-3'). PCR products were resolved on a 2 % agarose gel and
 165 sequence-confirmed.

166

167 **2.5-Electrophoretic mobility shift assays (EMSA)**

168 *Zic2* and *Cdx1* binding to *Pax3*NCE2 sequences was assessed essentially as previously described [26].
 169 Briefly, binding reactions were carried out in a previously described *Zic* binding buffer [41] with 8µg
 170 of nuclear extracts from mock-, _{HA}*Zic2* or _{FLAG}*Cdx1* transfected Cos7 cells. Supershift assay was
 171 performed using 1µg of rabbit anti-HA antibody (Abcam). Specificity of binding was assessed by
 172 competition with a 100-fold molar excess of unlabeled wild type or mutated cold probe. To test the
 173 interaction of *Cdx1* and *Zic2* in the presence of the target DNA, _{HA}*Zic2* and _{FLAG}*Cdx1* nuclear extracts
 174 were incubated for 30 min in *Zic* binding buffer at 4 °C before the addition of the radiolabelled probe
 175 (either *Pax3*NCE2 CdxBS1, CdxBS3 or *Zic*BS). The sense strand of each wild type double-stranded
 176 probe was previously described [26]. The sense strand of a double-stranded probe harbouring the
 177 mutated *Pax3*NCE2 *Zic*BS was as described above for site-directed mutagenesis. The sense strand of a
 178 double stranded probe harbouring a previously described *Zic*BS [41] (used as positive control) was: 5'-
 179 GATCCTGTGATTTTCGTCTTGGGTGGTCTCCCTCG-3' (with *Zic*BS underlined).

180
 181 **2.6-Western blot, co-immunoprecipitation and GST pull-down assays**

182 Primary antibodies and dilutions used for western blotting were: mouse anti-FLAG 1:1000 (M2,
 183 Sigma), rabbit anti-HA 1:2000 (ab9110, Abcam), mouse anti-Myc 1:100 (in house 9E10 hybridoma)
 184 and rabbit anti-GAPDH 1:2500 (sc25778, Santa Cruz Biotech).

185 For co-immunoprecipitation, Cos7 cells were transfected with expression vectors for _{FLAG}*Cdx1* and
 186 _{HA}*Zic2* using Genejuice transfection reagent (Novagen) and harvested in immunoprecipitation buffer
 187 (25 mM Hepes, pH 7.2, 0.5% Nonidet P-40, 150 mM NaCl, supplemented with protease inhibitors).
 188 Immunoprecipitations and western blots were carried out as previously described [33].

189 For pull-down assays, Glutathione *S*-transferase (GST)-*Cdx1*, GST-*Cdx1* homeodomain (GST-
 190 *Cdx1*Homeo) and GST-*Cdx1* N-terminus (GST-*Cdx1*Nterm) fusion proteins were produced and
 191 purified with glutathione-agarose beads (Sigma) as previously described [33]. FLAG-tagged full-length
 192 and deletion mutant *ZIC2* proteins were *in vitro* synthesized using the T_{NT} T7 quick coupled
 193 transcription/translation system (Promega) and previously described plasmids [34]. *In vitro* pull-down
 194 assays were performed as previously described [33] and interactions were revealed by western blotting
 195 using mouse anti-FLAG M2 antibody (Sigma). To test the interaction between *ZIC2* and *Cdx1* in the
 196 presence of NCE2 sequences, *in vitro* synthesized _{FLAG}*ZIC2* proteins were pre-incubated with
 197 increasing amounts of NCE2 DNA (50 or 200 ng) for 30 min in the same conditions as described for
 198 EMSA before adding GST or GST-*Cdx1* homeodomain fusion proteins.

199
 200 **2.7-Cell culture, transfections and RT-PCR analyses**

201 P19, Neuro2a (N2a) and Cos7 cell lines were propagated and transfected as previously described using
 202 Genejuice reagents (Novagen) in accordance with manufacturer's protocol [26].

203 Luciferase reporter assays were performed essentially as previously described [26]. For *Zic2* or *Sox2*
 204 dose response assays, N2a (8x10⁴ cells per well) and P19 (3x10⁴ cells per well) were transfected with
 205 100 ng of *Pax3*NCE2-Luciferase reporter construct alone or with increasing amounts of _{HA}*Zic2* (10 ng
 206 to 40 ng) or _{Myc}*Sox2* (10 ng to 75 ng) expression vectors. For analysis of the synergistic effect of *Cdx1*
 207 and *Zic2*, N2a cells were transfected with 100 ng of wild type or mutated *Pax3*NCE2-Luciferase
 208 reporter construct alone, or with fixed amount of _{FLAG}*Cdx1* (5ng) and/or _{HA}*Zic2* (10 ng) expression

209 vectors. When required, an empty expression vector was also included to complete the final amount of
 210 DNA per well to 150 ng. For analysis of the synergistic transactivation of *Pax3*NCE2 by Cdx1, Zic2
 211 and Sox2 co-expression, fixed amounts of FLAGCdx1 (10 ng), _{HA}Zic2 (40 ng) and _{Myc}Sox2 (50 ng) were
 212 used and an empty expression vector was also included to ensure a total of 200 ng of DNA per well.
 213 All transfections were performed at least five times in triplicate. In all experiments, specificity of
 214 NCE2 activation was assessed by using a previously described luciferase reporter construct consisting
 215 of the *Pax3* 150bp minimal promoter alone [26], as a negative control. Forty-eight hours after
 216 transfection, cells were disrupted in 100 µl of lysis buffer (0.1 M Tris [pH 8.0], 1% Igepal, 1 mM
 217 dithiothreitol) and assessed for luciferase activity with a Berthold LB9507 luminometer (Berthold
 218 Technologies). Expression of exogenous FLAGCdx1, _{HA}Zic2 and _{Myc}Sox2 in cell lysates was verified by
 219 western blot.

220 To modulate Zic2 activity, N2a cells were seeded in 100-mm tissue culture plates (2x10⁶ cells per
 221 plate) and transiently transfected with increasing doses (3, 6 and 9 µg) of _{HA}Zic2-IRES-GFP expression
 222 vector. Forty-eight hours after transfection, GFP-positive cells were recovered by FACS and analyzed
 223 by RT-PCR (for *Pax3* and *Gapdh* expression) as well as via western blot (for _{HA}Zic2 and *Gapdh*
 224 expression).

225 For dose-response analyses of Shh-induced repression of *Pax3*, *Zic2* and *Zic5* expression, N2a cells
 226 were seeded in 6 well plates (4x10⁵ cells per well) and treated the following day with varying doses
 227 (50-200 ng/ml) of recombinant mouse Shh-N proteins (R&D systems) in absence or presence of
 228 1ug/ml cyclopamine (R&D systems). Cells were harvested 24h post-treatment and analyzed by RT-
 229 PCR.

230 For cycloheximide (CHX) treatments, N2a cells were pre-treated for 30 min with 30 µg/mL of CHX or
 231 with the vehicle (DMSO) alone as previously described [26] and then treated for 24h with or without
 232 Shh-N recombinant protein (200 ng/mL) in the presence of 1 µg/mL of CHX.

233 For rescue experiments, N2a cells were seeded in 100-mm tissue culture plates (2x10⁶ cells per plate)
 234 and transiently transfected with _{HA}Zic2-IRES-GFP or empty IRES-GFP expression vectors. The
 235 following day, cells were incubated in the presence of Ctl or Shh-enriched (200 ng/ml) medium and
 236 cultured for another 24h prior to recovery of GFP-positive cells by FACS.

237 RNA isolation and RT-PCR analyses were performed as previously described [26]. The primers used in
 238 this study were: *Pax3* (forward: 5'-CCTGCCAACATACCAGCTGTCG-3', reverse: 5'-
 239 CTGAGGTGAAAGGCCATTGCCG-3'); *Zic2* (forward:5'-AAGGTCTTCGCACGCTCCGAG-3',
 240 reverse: 5'-CGCAACGAGCTGGGATGCGTGT-3'); *Zic5* (forward: 5'-
 241 CAAGATCCACAAGCGCACTCATAACA-3', reverse: 5'-TTGGGTCCAGCACAGGGGACAAAG-
 242 3'); *Gapdh* (forward: 5'-TCCTGCACCACCAACTGCTTAGC-3', reverse: 5'-
 243 AGGTCCACCACCCTGTTGCTGTA-3').

244

245 **2.8- Statistical analyses**

246 Statistical analyses were performed using GraphPad Prism software version 5.0. Differences between
 247 means were evaluated by one way ANOVA followed by a Tukey's post test and classed as not
 248 significant (n.s., $p>0.05$) or significant (*, $p<0.05$; **, $p<0.01$; ***, $p<0.001$).

249

250

251 **3-RESULTS**

252

253 ***3.1-A positive Cdx input is necessary but not sufficient to refine the Pax3 expression domain in the***
254 ***caudal neuroectoderm***

255 *Cdx* genes (*Cdx1/2/4*) encode homeodomain transcription factors exhibiting functional redundancy and
 256 overlapping expression patterns in the caudal embryo [42-48]. Using mouse transgenic reporters and
 257 murine cell line perturbation analyses, we have previously demonstrated that Cdx proteins are required,
 258 downstream of canonical Wnt signaling, to induce *Pax3* expression in the mouse caudal neuroectoderm
 259 [26]. However, as shown in Fig.1A by immunofluorescence analysis of Cdx2 and *Pax3* distribution in
 260 e9.5 caudal NT sections, *Cdx* and *Pax3* expression patterns only partially overlap [1, 42, 44, 45].
 261 Indeed, Cdx proteins are broadly distributed in the entire tailbud and, more anteriorly, they are detected
 262 along the whole DV axis of the recently closed NT. In contrast, *Pax3* expression is restricted to the
 263 lateral borders of the open PNP and, more anteriorly, to the dorsal NT. This implies that non-Cdx
 264 inputs are required to refine the *Pax3* expression domain in the caudal neuroectoderm and leaves us
 265 with three possibilities that may involve either one or two mechanisms (Fig.1B). The first possibility
 266 (Mechanism-1 only) would involve one or several Cdx cofactors that exhibit more-or-less restricted
 267 neural expression in the lateral PNP and dorsal NT. The second possibility (Mechanism-2 only) would
 268 involve a negative input from a repressor expressed in the medial PNP and ventral NT. The third
 269 possibility would involve a combination of both mechanisms.

270

271 ***3.2-The neural and dorsally restricted zinc finger transcription factor Zic2 regulates Pax3***
272 ***expression***

273 Based on their overlapping expression pattern with Cdx and *Pax3*, we first hypothesized that *Zic2/5*
 274 transcription factors might contribute to Mechanism-1. Indeed, *Zic* proteins can transactivate target
 275 genes and of the five murine *Zic* genes, only the *Zic2-Zic5* gene pair (sharing the same 5'-flanking
 276 region) is expressed in the caudal most region of the neuroectoderm [10]. Moreover, *Pax3* expression
 277 has been previously reported to be significantly reduced in NCC homozygous for a knockdown allele
 278 of *Zic2* while *Zic2*-null mutants exhibit posterior NT and NCC defects that phenocopy those observed
 279 in *Pax3*-null mutants [12]. To validate the candidacy of *Zic2* as a *Pax3* regulator, we began by carrying
 280 out a detailed analysis of their expression pattern using whole-mount *in situ* hybridization in stage-
 281 matched e9.0 and e9.5 mouse embryos. In accordance with previous studies, this analysis revealed a
 282 striking and extensive overlap in the neural expression domain of both genes along the AP axis
 283 (Fig.2A-J). Interestingly, as evidenced by its more posterior limit of expression in the open PNP, this
 284 analysis notably demonstrated that *Zic2* is in fact induced earlier than *Pax3* in the caudal embryo
 285 (compare Figs.2C,E,G with 2D,F,H). Following NT closure, *Pax3* and *Zic2* are then found to be
 286 equally expressed in a dorsal domain that covers ~40% of the DV neural axis (bracket in Fig.2I-J). It is
 287 noteworthy that such overlapping expression pattern is neural specific since, outside the NT, *Pax3* and
 288 *Zic2* are expressed in a mutually exclusive manner in the somites (asterisk in Fig.2I,J). Thus, these data
 289 support the candidacy of *Zic2* and further suggest that it might be involved in both the induction and
 290 dorsal restriction of neural *Pax3* expression. To more formally test our hypothesis that *Zic2* regulates
 291 *Pax3* expression, we then overexpressed *Zic2* in the murine NCC-derived N2a cell line and evaluated
 292 the effect on *Pax3* expression by RT-PCR. As shown in Fig.2K, overexpression of *Zic2* resulted in a

293 specific and dose-dependent increase of *Pax3* expression. In summary, our data strongly suggest that
 294 *Zic2* is a regulator of *Pax3* expression.

295

296 **3.3-Zic2 directly binds and transactivates Pax3NCE2**

297 We previously showed that the *Pax3*NCE2 CRM is sufficient for recapitulating induction and dorsal
 298 restriction of *Pax3* expression in the caudal neuroectoderm [26]. As we hypothesised that *Zic2* is a Cdx
 299 neural cofactor, we reasoned that *Zic2* should be able to activate *Pax3* expression via this Cdx-
 300 dependent CRM. We tested this possibility via luciferase assays in N2a cells and found that *Zic2*
 301 transactivated a *Pax3*NCE2 reporter in a dose-dependent manner, similarly to endogenous *Pax3*
 302 (Fig.3A and 2K). EMSAs were then used to determine whether *Zic2* directly binds to *Pax3*NCE2. *Zic*
 303 proteins are known to bind GC-rich elements but very few *Zic*BS have been previously identified in
 304 CRMs of *Zic*-regulated genes [10]. Thus, to avoid excluding any unpredicted binding site, we scanned
 305 the whole NCE2 sequence with eight previously described overlapping probes [26]. This approach
 306 revealed that one of these probes was bound by *Zic2* as efficiently as a probe containing a previously
 307 described *Zic*BS [41] (Fig.3B). We confirmed the presence of _{HA}*Zic2* in the complex formed with the
 308 NCE2 probe by supershift with an anti-HA antibody (Fig. 4E'). In accordance with previous reports,
 309 sequence analysis of the NCE2 probe revealed the presence of a GC-rich 9-nucleotide core sequence
 310 (5'-CTGCTGGGG-3'). Mutation of guanosine residues in position 6 and 7 prevented *Zic2* binding to a
 311 cold probe bearing these point mutations, thus demonstrating specificity of *Zic2* binding to this NCE2
 312 target sequence (Fig.4E'). We next sought to determine whether *Zic2*, like Cdx proteins, occupies the
 313 endogenous *Pax3*NCE2 using ChIP-PCR. To this end – and because we failed to obtain a ChIP-grade
 314 anti-*Zic2* antibody – we overexpressed _{HA}*Zic2* in N2a cells and evaluated its presence on NCE2 using
 315 anti-HA. _{FLAG}Cdx1-overexpressing cells were used for comparison purposes. As shown in Fig.3C,
 316 *Pax3*NCE2 was specifically amplified in sonicated chromatin samples immunoprecipitated with either
 317 anti-HA or anti-FLAG antibodies, while no amplification was obtained when a mouse pre-immune
 318 serum was used for IP. Altogether, these results demonstrate that *Zic2* directly binds and transactivates
 319 *Pax3*NCE2.

320

321 **3.4-Zic2 directly interacts with Cdx1**

322 Analysis of NCE2 sequences revealed that the *Zic*BS is flanked by CdxBS in close proximity (Fig.5B),
 323 further supporting a putative Cdx cofactor function for *Zic2*. To directly test this possibility, we carried
 324 out protein-protein interaction assays beginning with co-IP in _{HA}*Zic2*- and/or _{FLAG}Cdx1-transfected
 325 Cos7 cells. As shown in Fig.4A, mouse *Zic2* was found to specifically interact with Cdx1 when both
 326 are co-expressed. Then, to assess whether this interaction was direct, we performed GST-based pull-
 327 down assays using *in vitro* translated FLAG-tagged human ZIC2 and bacterially produced GST fusion
 328 proteins containing either the full-length Cdx1, the Cdx1 homeodomain or the Cdx1 N-terminal domain
 329 (GST-Cdx1, GST-Cdx1Homeo and GST-Cdx1Nterm). Western blotting using an anti-FLAG antibody
 330 showed that _{FLAG}ZIC2 directly interacts with both the full-length Cdx1 and the Cdx1 homeodomain
 331 whereas no interaction was observed with the Cdx1 N-terminus (Fig.4B). Mapping of Cdx1 and ZIC2
 332 interacting domains was next assessed using a series of *in vitro* translated _{FLAG}ZIC2 deletion-containing
 333 proteins and the GST-Cdx1Homeo fusion protein (Fig.S1A). This analysis revealed that ZIC2 and
 334 Cdx1 interact via their respective DNA binding domain since no interaction with the Cdx1

335 homeodomain was observed when the Zinc finger domain of ZIC2 was deleted (construct 1-255)
 336 (Fig.4C-D and Fig.S1B). Regions located N-terminus (constructs 140-532 and 255-532) or C-terminus
 337 (1-415) to the Zinc finger domain have apparently no major impact on this interaction (Fig.4C-D).
 338 Intrigued by this discovery, we then tested whether Zic2 and Cdx1 could still physically interact with
 339 each other in the presence of their respective target sequences using EMSA as well as GST pull-down
 340 assays. In EMSA, we found that pre-incubation of _{HA}Zic2- with _{FLAG}Cdx1-expressing Cos7 nuclear
 341 extracts did not preclude target DNA binding and even resulted in the appearance of novel bands of
 342 higher molecular weight either on the ZicBS (E'), the CdxBS1 (E'') or the CdxBS3 (E'''), suggesting
 343 the formation of a Zic2-Cdx1-DNA complex on these elements. Consistent with these outcomes, pre-
 344 incubation of _{FLAG}ZIC2 with increasing amounts of the whole NCE2 did not impair its interaction with
 345 the Cdx1 homeodomain in GST pull-down assays (Fig.S1C). These data demonstrate that, although the
 346 Zic2-Cdx1 physical interaction is mediated by their respective DNA binding domain, this does not
 347 prevent the ability of both Zic2 and Cdx1 to bind their respective target sequences.

348

349 ***3.5-Robust Zic2 and Cdx1 functional interaction on Pax3NCE2 requires a positive input from the*** 350 ***neural specific Sox2 transcription factor***

351 Last validation of Zic2 as a Cdx1 cofactor required the demonstration of a functional interaction with
 352 Cdx1 and we assessed this via luciferase assays in both N2a and undifferentiated P19 cell lines. In N2a
 353 cells, Cdx1-Zic2 co-expression resulted in a weak synergistic activation of the *Pax3NCE2* luciferase
 354 reporter (Fig.5A). Interestingly, mutation of the three functional CdxBS alone or in combination with
 355 mutation of the ZicBS significantly abrogated this Cdx1-Zic2 cooperative effect. This is consistent with
 356 the central role of Cdx1 in activation of *Pax3NCE2* [26] and suggests that binding of Cdx1 to this
 357 CRM is important for the Cdx1-Zic2 functional interaction. Intriguingly, although mutation of the
 358 ZicBS also abrogated the Cdx1-Zic2 cooperative effect, these analyses further revealed that Zic2 ability
 359 to transactivate *Pax3NCE2* can be independent of the ZicBS as well as the three CdxBS (Fig.5A).
 360 Moreover, in the undifferentiated P19 cell line, Zic2 failed to transactivate *Pax3NCE2* and no
 361 cooperative effect between Cdx1 and Zic2 was observed (data not shown). Therefore, this suggests that
 362 interaction with another neural factor is necessary for the Zic2-Cdx1 complex to robustly transactivate
 363 *Pax3NCE2*. Based on several lines of evidence, Sox2 quickly emerged as a primary candidate in this
 364 regard. Indeed, at least one potential SoxBS is present in *Pax3NCE2* (Fig.5B), SoxB1 family members
 365 have recently been implicated as positive regulators of *Pax3* expression [30] and the SoxB1 family
 366 member Sox2 has been shown to directly interact with Cdx1 [33]. To assess the putative contribution
 367 of Sox2, we first evaluated whether this transcription factor alone was able to transactivate the
 368 *Pax3NCE2* luciferase reporter in N2a cells. Consistent with our hypothesis, Sox2 strongly
 369 transactivated *Pax3NCE2* in a dose-dependent manner (Fig.5C). Of note, such effect was not observed
 370 in P19 cells, suggesting that the Sox2 capacity to transactivate this CRM relies on the presence of
 371 other, as yet undefined, neural factors (Fig.5C). To demonstrate the importance of the Sox2 input in the
 372 functional interaction between Cdx1 and Zic2, we co-transfected N2a cells with Cdx1, Zic2 and Sox2
 373 and evaluated the activation of the *Pax3NCE2* luciferase reporter. Interestingly, a significant
 374 synergistic effect was observed when the three factors were co-expressed (Fig.5D; see Fig.S2 for
 375 western blot validations). Together, these results suggest that *Pax3NCE2* is robustly activated by a
 376 concerted interaction between Cdx1, Zic2, and Sox2 trans-acting factors.

377

378 **3.6-Zic2 is a potential mediator of the Shh-induced repression of Pax3**

379 Having confirmed that *Zic2* is a *bona fide* Cdx cofactor, and thus contribute to Mechanism-1, we next
 380 investigated the possibility that it could also contribute to the repressor-dependent Mechanism-2
 381 (Fig.1B). Indeed, a ventrally Shh-induced repressive pathway is a prominent candidate to consider and
 382 both *Zic* members and *Pax3* are known to be affected by such regulatory cascade. Studies in multiple
 383 species, including mice, indicate that Shh signals secreted by the notochord and floorplate are required
 384 to prevent ectopic expression of *Pax3* and *Zic* members in the ventral NT [20, 21, 25, 30, 49-51]. While
 385 the molecular mechanism of this regulation is poorly understood for *Zic* members, recent work in
 386 zebrafish and chick embryos suggest that the Shh target Nkx6.1 represses *Pax3* expression via direct
 387 binding to a *Pax3* CRM located in the 4th intron [29, 30]. However, whether such Shh-Nkx6.1 circuit is
 388 at work in the mouse and active at all AP levels has not been investigated. To verify this, we compared
 389 the expression profile of *Pax3* and *Zic2* with the distribution of Nkx6.1 proteins in the caudal
 390 neuroectoderm of stage matched e9.5 mouse embryos (Fig.6A-O). Surprisingly, we found that Nkx6.1
 391 is not detected in the open PNP and recently closed NT whereas *Pax3* is already induced and properly
 392 restricted in these structures (compare Fig.6A-B with K-L). Therefore, the Shh-Nkx6.1 pathway cannot
 393 be responsible for the restriction of *Pax3* expression in the caudal neuroectoderm of mouse embryos.
 394 On the other hand, we found that *Zic2* is dynamically expressed along the DV axis of the caudal
 395 neuroectoderm. *Zic2* transcripts are indeed first detected in the whole PNP and along the entire DV axis
 396 of the recently closed NT before becoming dorsally restricted more anteriorly (Fig.6F-J). In more
 397 anterior regions, a perfect overlap is finally observed between *Zic2* and *Pax3* neural expression
 398 domains (Fig.2I-J). Very interestingly, we also noticed that the onset of *Zic2* repression in the ventral
 399 NT is correlated with the onset of Nkx6.1 expression (see arrow in Fig.6H and M). On one hand, all
 400 these observations suggest that, while the Cdx-Zic2 neural input is necessary for *Pax3* induction, a
 401 Shh-Nkx6.1-independent input must also be required to restrict *Pax3* expression in the open PNP and
 402 most caudal NT. On the other hand, these expression data also strongly suggest that *Zic2* might be an
 403 intermediary in the mechanism of *Pax3* repression by the Shh-Nkx6.1 pathway. We sought to validate
 404 this hypothesis using the murine N2a cell line and first validated this line as a good model to study the
 405 mechanism of *Pax3* repression by Shh (Fig.S3). We then performed a dose-response assay to evaluate
 406 whether *Zic2* and *Pax3* were both repressed by increasing doses of Shh (Fig.6P). As expected from
 407 previous work [20, 21, 25, 30, 49-51], Shh repressed the expression of *Pax3* as well as expression of
 408 the *Zic2-Zic5* gene pair. To finally confirm our hypothesis, we tried to rescue *Pax3* expression by
 409 overexpressing *Zic2* in Shh-treated cells. In agreement with a *Zic*-dependent mechanism, transfection
 410 with a *Zic2* expression vector specifically rescued *Pax3* expression from the repressive input of Shh
 411 (Fig.6Q). Taken together, these evidences strongly support an intermediary role for *Zic2* in the
 412 mechanism of *Pax3* repression by Shh in the mouse.

413

414 **4-DISCUSSION**

415

416 In this work, we report a novel direct role for *Zic2* in the regulation of *Pax3* neural expression. Our
 417 data indicate that *Zic2* can transactivate *Pax3* at least via the NCE2 CRM, which we previously showed
 418 to be sufficient for recapitulating caudal *Pax3* expression in pre-migratory NCC and dorsal NT [26].

419 Interestingly, we also provide evidence that *Zic2* is involved in both the Wnt-mediated induction (by
 420 interacting with Cdx proteins) and the Shh-induced dorsal restriction (by being itself repressed by Shh
 421 signals) of *Pax3* expression. Therefore, our studies provide important mechanistic insights into how AP
 422 and DV instructive cues can be coordinately integrated on a short CRM.

423

424 **4.1-Role of the *Zic2-Cdx* complex in Wnt-mediated induction of *Pax3* neural expression**

425 In previous studies, we presented evidence that a Wnt-Cdx circuit is critically required for activation of
 426 a *Pax3*NCE2 reporter in transgenic mice [26]. These data support a model in which Cdx proteins
 427 convey the posteriorizing Wnt- β Catenin signals to *Pax3* in order to mediate induction of trunk NCC
 428 [26, 52, 53]. Interestingly, indirect activation of *Pax3* expression by canonical Wnt signaling –
 429 involving either AP2a or Gbx2 as intermediates – has also been described in *Xenopus* embryos during
 430 induction of cranial NCC [17, 54]. On the other hand, other groups have in addition reported that *Pax3*
 431 could be directly regulated by Wnt- β Catenin signaling through CRMs distinct from NCE2 [29, 30, 55].
 432 This suggests that regulation of *Pax3* expression by the canonical Wnt pathway could be controlled via
 433 both direct and indirect means in order to buffer against perturbations in the Wnt input. In the caudal
 434 neuroectoderm, a third level of regulation would even be possible given that Cdx proteins can directly
 435 and positively interact with the β catenin-Lef/Tcf complex on Lef/Tcf binding sites [33]. However, the
 436 very broad distribution of Cdx proteins in both neural and non-neural cells of the caudal embryo [42,
 437 56] implies that other players must cooperate with the Wnt-Cdx inductive input to spatially refine the
 438 *Pax3* expression domain.

439 The present study demonstrates that *Zic2* not only acts as a *Pax3* regulator, but also as a neural-specific
 440 Cdx cofactor. Indeed, we found that *Zic2* and Cdx1 cooperate in the activation of *Pax3*NCE2 and
 441 physically interact via their respective DNA binding domain (Fig.4 and 5). Such involvement of DNA
 442 binding domains in protein-protein interactions is not unusual and examples implicating either the *Zic2*
 443 C2H2 zinc finger region or the Cdx1 homeodomain have been previously described [33, 34]. On the
 444 other hand, to the best of our knowledge, this is the first report showing that the *Zic* zinc finger region
 445 or the Cdx homeodomain can simultaneously mediate protein-protein as well as protein-DNA
 446 interactions (Fig.4, 5 and Fig.S1). This bifunctionality is most likely due to the fact that, for each of
 447 these proteins, establishment of direct contacts with DNA bases is not carried out by the whole DNA
 448 binding domain *per se* but by specific subregions only. Indeed, previous studies have suggested that
 449 only zinc fingers 3-5 of *Zic2* might be implicated in DNA recognition [10, 57, 58] whereas, for
 450 homeodomain proteins, DNA binding activity is known to be specifically conferred by the 3rd α -helix
 451 [59]. Thus, this suggests that the *Zic2-Cdx1* interaction might be mediated by the zinc fingers 1-2 of
 452 *Zic2* and the 1st and/or 2nd α -helix of the Cdx1 homeodomain. Regardless of the exact minimal
 453 interacting domain on each protein, it should be noted that functional interactions between different
 454 members of each family are expected given the very high conservation of both *Zic* and Cdx DNA
 455 binding domains [58, 60].

456 Interestingly, our data also indicate that, although both *Zic2* and Cdx1 have the ability to bind
 457 *Pax3*NCE2 sequences in a direct as well as in an indirect manner (Fig.4), robust activation by the *Zic2*-
 458 Cdx1 complex requires direct binding of each protein to this CRM as well as the participation of Sox2
 459 (Fig.5) – a previously described Cdx interacting partner [33]. Such contribution of Sox2 is in line with
 460 recent work suggesting the implication of SoxB members in the regulation of neural *Pax3* expression

461 via another CRM located in the 4th intron [30]. On the other hand, it is interesting to note that in
 462 contrast to Cdx proteins [26], neither *Zic2* nor *Sox2* can activate *Pax3* expression in non-neural cells
 463 (Fig.5C and data not shown). Taken together with the indispensable role of CdxBS1-3 for *Pax3*NCE2
 464 activity [26], this strongly suggests that Cdx proteins have a pioneer-like activity required to attract and
 465 tether neural-specific transcriptional activators on this CRM [61]. Interestingly, a similar pioneer-like
 466 activity has been also previously suggested for Cdx2 in the regulation of the transcriptional program of
 467 intestinal epithelial cells [62] as well as for Pdx1 – another member of the Cdx-containing paraHox
 468 family – in the regulation of several genes important for pancreatic β cell development and function
 469 [63, 64].

470

471 **4.2-Restriction of *Pax3* expression to the lateral borders of the PNP and the dorsal NT**

472 A role for notochord- and floor plate-secreted Shh in the regulation of *Pax3* restriction in the dorsal NT
 473 has been described in diverse model organisms [20, 30, 65]. In the mouse, Shh gain-of-function in
 474 *Ptch1*-null mutants results in a nearly complete loss of *Pax3* expression whereas Shh loss-of-function
 475 in Shh-null embryos results in expansion of *Pax3* expression along the entire DV neural axis [21, 66].
 476 Recent studies suggest that this Shh-induced repressive input could be mediated by the Nkx6.1
 477 homeodomain transcriptional repressor – a known direct target of the Shh-Gli pathway [67]. Indeed,
 478 Moore et al. [30] reported that Nkx6.1 can directly bind a *Pax3* CRM located in intron-4 (called CNE3)
 479 and that mutation of a putative binding site for homeodomain proteins within this CRM is required to
 480 turn on ubiquitous but mosaic expression of a reporter gene driven by this CRM in zebrafish embryos.
 481 Combination of this work with Tcf3 ChIP-seq data from ES cells [68] led these authors to propose a
 482 model whereby Shh-induced Nkx6.1 could counteract canonical Wnt signaling in order to restrict
 483 induction of *Pax3* expression to the lateral borders of the PNP [30]. However, in addition to the fact
 484 that Tcf3 is not a direct mediator of Wnt- β Catenin positive inputs [69], this model is not consistent
 485 with the Nkx6.1 expression profile in the mouse. Indeed, we and others have shown that Nkx6.1 is not
 486 expressed in the open PNP and recently closed NT, whereas *Pax3* is already induced and properly
 487 restricted in these regions (Fig.6) [67]. Moreover, *in situ* hybridization analyses have failed to detect
 488 *Shh* transcripts in the caudal neuroectoderm [70], implying that no other Shh targets could be involved
 489 in this mechanism. In agreement with this, *Zic2*, a known Shh-regulated gene in the mouse [49], is
 490 broadly expressed in the entire PNP and recently closed NT (Fig.6). Taking into account all these
 491 observations, the proposed Shh-Nkx6.1 repressive circuit cannot contribute to the induction phase of
 492 *Pax3* expression and can only be implicated in the maintenance of *Pax3* dorsal restriction.

493 Interestingly, our data indicate that an alternative pathway involving repression of the *Pax3* activator
 494 *Zic2* could also mediate the Shh-induced repression of *Pax3* expression (Fig.6). This hypothesis is
 495 strongly supported by data from Moore et al. [30] showing that Nkx6.1 overexpression has a much
 496 more dramatic impact on repression of *Pax3* expression in comparison to the CNE3 reporter bearing
 497 the mutated homeodomain binding site. Moreover, our expression data in Fig.6 – showing that the
 498 onset of *Zic2* repression is correlated with the onset of Nkx6.1 expression in the ventral NT – are also
 499 consistent with the idea that *Zic2* might be a direct target of Nkx6.1. Although it is currently highly
 500 speculative, we propose that this alternative Shh-Nkx6.1-Zic2-Pax3 pathway targeting NCE2 would be
 501 functionally redundant with the more straightforward Shh-Nkx6.1-Pax3 pathway targeting CNE3 [30].
 502 Given the co-expression of the *Zic2-Zic5* gene pair as well as the known functional redundancy

503 between Zic members [4, 71-74], we also believe that Zic5 acts redundantly with Zic2 in this
 504 mechanism. Furthermore, given that Zic and Gli proteins have similar DNA binding specificity and Zic
 505 inhibit Gli transcriptional activity [41], it is tempting to speculate that cross-repression between Zic2/5
 506 and the Shh pathway would be important for proper DV patterning of the NT.

507

508 **4.3-Coordinated integration of AP and DV instructive cues and redundancy between Pax3 CRMs**

509 As evidenced by our work and the work of others, *Pax3* gene expression is regulated by two sets of
 510 CRMs that are clustered in the 5'-flanking region or in intron-4, respectively (Fig.5B) [18, 26-30, 55].
 511 Interestingly, although the requirement of intron-4 CRMs has not yet been formally addressed via gene
 512 targeting approaches, deletion of 5'-located CRMs in the mouse is indicative of functional redundancy
 513 between each regulatory cluster [29]. It is also interesting to note that, although each set of CRMs is
 514 expected to respond to the same AP and DV instructive cues, different mechanisms appears to be used
 515 (e.g. Shh-Nkx6.1-Pax3 vs Shh-Nkx6.1-Zic2-Pax3) and different complementarities are seen among
 516 CRMs of each cluster. Within the 5' cluster, NCE1 and NCE2 appear to be complementary for the
 517 spatial control of *Pax3* expression along the AP axis. Indeed, while we have shown that NCE2 drives
 518 reporter gene expression in a caudal-specific and Cdx-dependent manner, others have shown that
 519 NCE1 is involved in the regulation of cranial *Pax3* expression in a Pbx1-dependent manner [26, 75]. In
 520 contrast, within the intron-4 cluster, CNE3 (also known as ECR2 or IR1) and CNE1 (also known as
 521 IR2) appear to exhibit temporal complementarities in the control of *Pax3* expression, with CNE3
 522 suggested to be involved in the induction phase in a Lef/Tcf-dependent manner and CNE1 suggested to
 523 be involved in the maintenance phase in a Pax3/7-dependent manner [18, 29, 30]. In accordance with
 524 the key developmental role of Pax3, such functional redundancy at both the *cis* and *trans* level most
 525 likely allows to protect its expression from the otherwise deleterious impacts of genetic mutations in *cis*
 526 or perturbations of signaling pathways in *trans*.

527 Our work on NCE2 indicates that it may serve as a good model to further understand how AP and DV
 528 instructive cues can be coordinately integrated on a single CRM. Indeed, in addition to allow
 529 recapitulating induction of *Pax3* expression in the PNP, NCE2-driven expression is properly restricted
 530 [26]. It is also noteworthy that we and others have shown that NCE2 seems particularly enriched in
 531 binding sites for a wide array of transcription factors including members of the Cdx, Pou class-III,
 532 SoxB, Zic and Tead families [26, 28, 31]. In an effort to gather all this information into a dynamic
 533 network (Fig.7), we propose a model in which the posteriorizing cue from the Wnt-Cdx circuit, in
 534 cooperation with Zic and SoxB positive inputs, is first required to induce *Pax3* expression in the PNP.
 535 Later on (i.e. more rostrally), the Shh-Nkx repressive input is then most likely involved in the
 536 maintenance of the dorsally-restricted *Pax3* expression domain via repression of *Zic2/5* expression. In
 537 absence of Cdx factors more rostrally, maintenance is also most likely ensured by the positive input of
 538 other transcription factors such as members of the Pou class III and Tead families [28, 31]. While this
 539 model clearly allows understanding how the *Pax3*NCE2 CRM is regulated by AP instructive cues
 540 (Wnt-Cdx), this is much less clear regarding the integration of DV instructive cues. Indeed, our studies
 541 clearly show that an unknown Shh-independent factor is required during the induction phase in order to
 542 limit expression to the lateral borders of the PNP. More work will definitely be necessary for the
 543 identification of this key player, once again in accordance with the mechanisms described in Fig.1B.

544

545 **4.4-Conclusion**

546 This study allowed confirming the central role of Cdx proteins in the induction of *Pax3* neural
 547 expression as well as identifying novel molecular functions for Zic2 as a Cdx co-factor and activator of
 548 *Pax3* expression. By allowing extension of the list of transcription factors able to bind and transactivate
 549 *Pax3*NCE2, our work also suggests that this CRM behaves as a “super-enhancer” region.

550

551 **ACKNOWLEDGEMENTS:** The authors thank Denis Flipo (UQAM) for FACS analyses and
 552 assistance with confocal imaging. Jonathan Epstein, Sabine Tejpar, Jun Aruga, Mahmud Bani-Yaghoub
 553 and David Lohnes are thanked for kindly agreeing to provide expression vectors. This work was
 554 supported by a grant from the Canadian Institute for Health Research (CIHR grant number MOP-
 555 111130) to NP. OSF holds an Alexander-Graham-Bell scholarship from the Natural Science and
 556 Engineering Research Council (NSERC) of Canada. NP is a Fonds de la Recherche du Québec – Santé
 557 (FRQS) Junior2 scholar.

558

559 **REFERENCES**

560

- 561 [1] M.D. Goulding, G. Chalepakis, U. Deutsch, J.R. Erselius, P. Gruss, Pax-3, a novel murine DNA binding protein
 562 expressed during early neurogenesis, *Embo J*, 10 (1991) 1135-1147.
- 563 [2] C. Gaston-Massuet, D.J. Henderson, N.D. Greene, A.J. Copp, Zic4, a zinc-finger transcription factor, is
 564 expressed in the developing mouse nervous system, *Developmental dynamics : an official publication of the*
 565 *American Association of Anatomists*, 233 (2005) 1110-1115.
- 566 [3] T. Nagai, J. Aruga, S. Takada, T. Gunther, R. Sporle, K. Schughart, K. Mikoshiba, The expression of the mouse
 567 *Zic1*, *Zic2*, and *Zic3* gene suggests an essential role for Zic genes in body pattern formation, *Developmental*
 568 *biology*, 182 (1997) 299-313.
- 569 [4] T. Inoue, M. Hatayama, T. Tohmonda, S. Itohara, J. Aruga, K. Mikoshiba, Mouse *Zic5* deficiency results in
 570 neural tube defects and hypoplasia of cephalic neural crest derivatives, *Developmental biology*, 270 (2004)
 571 146-162.
- 572 [5] D.J. Epstein, M. Vekemans, P. Gros, Splotch (*Sp2H*), a mutation affecting development of the mouse neural
 573 tube, shows a deletion within the paired homeodomain of Pax-3, *Cell*, 67 (1991) 767-774.
- 574 [6] R. Auerbach, Analysis of the developmental effects of a lethal mutation in the house mouse, *J Exp Zoology*,
 575 127 (1954) 305–329.
- 576 [7] J. Li, K.C. Liu, F. Jin, M.M. Lu, J.A. Epstein, Transgenic rescue of congenital heart disease and spina bifida in
 577 Splotch mice, *Development*, 126 (1999) 2495-2503.
- 578 [8] J. Aruga, The role of Zic genes in neural development, *Mol Cell Neurosci*, 26 (2004) 205-221.
- 579 [9] A. Mansouri, A. Stoykova, M. Torres, P. Gruss, Dysgenesis of cephalic neural crest derivatives in Pax7-/-
 580 mutant mice, *Development*, 122 (1996) 831-838.
- 581 [10] C.S. Merzdorf, Emerging roles for zic genes in early development, *Dev Dyn*, 236 (2007) 922-940.
- 582 [11] P. Elms, P. Siggers, D. Napper, A. Greenfield, R. Arkell, Zic2 is required for neural crest formation and
 583 hindbrain patterning during mouse development, *Developmental biology*, 264 (2003) 391-406.
- 584 [12] T. Nagai, J. Aruga, O. Minowa, T. Sugimoto, Y. Ohno, T. Noda, K. Mikoshiba, Zic2 regulates the kinetics of
 585 neurulation, *Proceedings of the National Academy of Sciences of the United States of America*, 97 (2000) 1618-
 586 1623.
- 587 [13] A.H. Monsoro-Burq, E. Wang, R. Harland, Msx1 and Pax3 cooperate to mediate FGF8 and WNT signals
 588 during *Xenopus* neural crest induction, *Dev Cell*, 8 (2005) 167-178.
- 589 [14] L.A. Taneyhill, M. Bronner-Fraser, Dynamic alterations in gene expression after Wnt-mediated induction of
 590 avian neural crest, *Mol Biol Cell*, 16 (2005) 5283-5293.

- 591 [15] A.G. Bang, N. Papalopulu, C. Kintner, M.D. Goulding, Expression of Pax-3 is initiated in the early neural
592 plate by posteriorizing signals produced by the organizer and by posterior non-axial mesoderm, *Development*,
593 124 (1997) 2075-2085.
- 594 [16] A.G. Bang, N. Papalopulu, M.D. Goulding, C. Kintner, Expression of Pax-3 in the lateral neural plate is
595 dependent on a Wnt-mediated signal from posterior nonaxial mesoderm, *Dev Biol*, 212 (1999) 366-380.
- 596 [17] N. de Croze, F. Maczkowiak, A.H. Monsoro-Burq, Reiterative AP2a activity controls sequential steps in the
597 neural crest gene regulatory network, *Proceedings of the National Academy of Sciences of the United States of*
598 *America*, 108 (2011) 155-160.
- 599 [18] A.T. Garnett, T.A. Square, D.M. Medeiros, BMP, Wnt and FGF signals are integrated through evolutionarily
600 conserved enhancers to achieve robust expression of Pax3 and Zic genes at the zebrafish neural plate border,
601 *Development*, 139 (2012) 4220-4231.
- 602 [19] K.F. Liem, Jr., G. Tremml, H. Roelink, T.M. Jessell, Dorsal differentiation of neural plate cells induced by
603 BMP-mediated signals from epidermal ectoderm, *Cell*, 82 (1995) 969-979.
- 604 [20] M.D. Goulding, A. Lumsden, P. Gruss, Signals from the notochord and floor plate regulate the region-
605 specific expression of two Pax genes in the developing spinal cord, *Development*, 117 (1993) 1001-1016.
- 606 [21] L.V. Goodrich, L. Milenkovic, K.M. Higgins, M.P. Scott, Altered neural cell fates and medulloblastoma in
607 mouse patched mutants, *Science*, 277 (1997) 1109-1113.
- 608 [22] J. Ericson, S. Morton, A. Kawakami, H. Roelink, T.M. Jessell, Two critical periods of Sonic Hedgehog
609 signaling required for the specification of motor neuron identity, *Cell*, 87 (1996) 661-673.
- 610 [23] T. Sato, N. Sasai, Y. Sasai, Neural crest determination by co-activation of Pax3 and Zic1 genes in *Xenopus*
611 ectoderm, *Development*, 132 (2005) 2355-2363.
- 612 [24] A.H. Monsoro-Burq, R.B. Fletcher, R.M. Harland, Neural crest induction by paraxial mesoderm in *Xenopus*
613 embryos requires FGF signals, *Development*, 130 (2003) 3111-3124.
- 614 [25] J. Aruga, T. Tohmonda, S. Homma, K. Mikoshiba, Zic1 promotes the expansion of dorsal neural progenitors
615 in spinal cord by inhibiting neuronal differentiation, *Developmental biology*, 244 (2002) 329-341.
- 616 [26] O. Sanchez-Ferras, B. Coutaud, T. Djavanbakht Samani, I. Tremblay, O. Souchkova, N. Pilon, Caudal-related
617 homeobox (Cdx) protein-dependent integration of canonical Wnt signaling on paired-box 3 (Pax3) neural crest
618 enhancer, *J Biol Chem*, 287 (2012) 16623-16635.
- 619 [27] T.A. Natoli, M.K. Ellsworth, C. Wu, K.W. Gross, S.C. Pruitt, Positive and negative DNA sequence elements
620 are required to establish the pattern of Pax3 expression, *Development*, 124 (1997) 617-626.
- 621 [28] R.C. Milewski, N.C. Chi, J. Li, C. Brown, M.M. Lu, J.A. Epstein, Identification of minimal enhancer elements
622 sufficient for Pax3 expression in neural crest and implication of Tead2 as a regulator of Pax3, *Development*, 131
623 (2004) 829-837.
- 624 [29] K.R. Degenhardt, R.C. Milewski, A. Padmanabhan, M. Miller, M.K. Singh, D. Lang, K.A. Engleka, M. Wu, J. Li,
625 D. Zhou, N. Antonucci, L. Li, J.A. Epstein, Distinct enhancers at the Pax3 locus can function redundantly to
626 regulate neural tube and neural crest expressions, *Dev Biol*, 339 (2010) 519-527.
- 627 [30] S. Moore, V. Ribes, J. Terriente, D. Wilkinson, F. Relaix, J. Briscoe, Distinct Regulatory Mechanisms Act to
628 Establish and Maintain Pax3 Expression in the Developing Neural Tube, *PLoS genetics*, 9 (2013) e1003811.
- 629 [31] S.C. Pruitt, A. Bussman, A.Y. Maslov, T.A. Natoli, R. Heinaman, Hox/Pbx and Brn binding sites mediate Pax3
630 expression in vitro and in vivo, *Gene Expr Patterns*, 4 (2004) 671-685.
- 631 [32] W.A. Whyte, D.A. Orlando, D. Hnisz, B.J. Abraham, C.Y. Lin, M.H. Kagey, P.B. Rahl, T.I. Lee, R.A. Young,
632 Master transcription factors and mediator establish super-enhancers at key cell identity genes, *Cell*, 153 (2013)
633 307-319.
- 634 [33] M. Beland, N. Pilon, M. Houle, K. Oh, J.R. Sylvestre, P. Prinos, D. Lohnes, Cdx1 autoregulation is governed
635 by a novel Cdx1-LEF1 transcription complex, *Mol Cell Biol*, 24 (2004) 5028-5038.
- 636 [34] R. Pourebrahim, R. Houtmeyers, S. Ghogomu, S. Janssens, A. Thelie, H.T. Tran, T. Langenberg, K. Vleminckx,
637 E. Bellefroid, J.J. Cassiman, S. Tejpar, Transcription factor Zic2 inhibits Wnt/beta-catenin protein signaling, *The*
638 *Journal of biological chemistry*, 286 (2011) 37732-37740.
- 639 [35] Y. Koyabu, K. Nakata, K. Mizugishi, J. Aruga, K. Mikoshiba, Physical and functional interactions between Zic
640 and Gli proteins, *The Journal of biological chemistry*, 276 (2001) 6889-6892.

- 641 [36] M. Bani-Yaghoub, R.G. Tremblay, J.X. Lei, D. Zhang, B. Zurakowski, J.K. Sandhu, B. Smith, M. Ribecco-
642 Lutkiewicz, J. Kennedy, P.R. Walker, M. Sikorska, Role of Sox2 in the development of the mouse neocortex,
643 *Developmental biology*, 295 (2006) 52-66.
- 644 [37] M.H. Kaufman, *The Atlas of Mouse Development*, Academic Press, London, 1992.
- 645 [38] D.G. Wilkinson, In " *In Situ* Hybridisation. A Practical Approach.", in: I. Press (Ed.), New York, 1992.
- 646 [39] B. Coutaud, N. Pilon, Characterization of a novel transgenic mouse line expressing Cre recombinase under
647 the control of the Cdx2 neural specific enhancer, *Genesis*, (2013) 1-8.
- 648 [40] J. Jeong, A.P. McMahon, Growth and pattern of the mammalian neural tube are governed by partially
649 overlapping feedback activities of the hedgehog antagonists patched 1 and Hhip1, *Development*, 132 (2005)
650 143-154.
- 651 [41] K. Mizugishi, J. Aruga, K. Nakata, K. Mikoshiba, Molecular properties of Zic proteins as transcriptional
652 regulators and their relationship to GLI proteins, *J Biol Chem*, 276 (2001) 2180-2188.
- 653 [42] B.I. Meyer, P. Gruss, Mouse Cdx-1 expression during gastrulation, *Development*, 117 (1993) 191-203.
- 654 [43] J.G. Savory, N. Pilon, S. Grainger, J.R. Sylvestre, M. Beland, M. Houle, K. Oh, D. Lohnes, Cdx1 and Cdx2 are
655 functionally equivalent in vertebral patterning, *Dev Biol*, 330 (2009) 114-122.
- 656 [44] F. Beck, T. Erler, A. Russell, R. James, Expression of Cdx-2 in the mouse embryo and placenta: possible role
657 in patterning of the extra-embryonic membranes, *Dev Dyn*, 204 (1995) 219-227.
- 658 [45] L.W. Gamer, C.V. Wright, Murine Cdx-4 bears striking similarities to the *Drosophila* caudal gene in its
659 homeodomain sequence and early expression pattern, *Mech Dev*, 43 (1993) 71-81.
- 660 [46] J.G. Savory, M. Mansfield, F.M. Rijli, D. Lohnes, Cdx mediates neural tube closure through transcriptional
661 regulation of the planar cell polarity gene Ptk7, *Development*, 138 (2011) 1361-1370.
- 662 [47] E. van den Akker, S. Forlani, K. Chawengsaksophak, W. de Graaff, F. Beck, B.I. Meyer, J. Deschamps, Cdx1
663 and Cdx2 have overlapping functions in anteroposterior patterning and posterior axis elongation,
664 *Development*, 129 (2002) 2181-2193.
- 665 [48] J. van Nes, W. de Graaff, F. Lebrin, M. Gerhard, F. Beck, J. Deschamps, The Cdx4 mutation affects axial
666 development and reveals an essential role of Cdx genes in the ontogenesis of the placental labyrinth in mice,
667 *Development*, 133 (2006) 419-428.
- 668 [49] L.Y. Brown, A.H. Kottmann, S. Brown, Immunolocalization of Zic2 expression in the developing mouse
669 forebrain, *Gene expression patterns : GEP*, 3 (2003) 361-367.
- 670 [50] K.B. Rohr, S. Schulte-Merker, D. Tautz, Zebrafish zic1 expression in brain and somites is affected by BMP
671 and hedgehog signalling, *Mechanisms of development*, 85 (1999) 147-159.
- 672 [51] A.M. Holtz, K.A. Peterson, Y. Nishi, S. Morin, J.Y. Song, F. Charron, A.P. McMahon, B.L. Allen, Essential role
673 for ligand-dependent feedback antagonism of vertebrate hedgehog signaling by PTCH1, PTCH2 and HHIP1
674 during neural patterning, *Development*, 140 (2013) 3423-3434.
- 675 [52] N. Pilon, K. Oh, J.R. Sylvestre, N. Bouchard, J. Savory, D. Lohnes, Cdx4 is a direct target of the canonical
676 Wnt pathway, *Dev Biol*, 289 (2006) 55-63.
- 677 [53] N. Pilon, K. Oh, J.R. Sylvestre, J.G. Savory, D. Lohnes, Wnt signaling is a key mediator of Cdx1 expression in
678 vivo, *Development*, 134 (2007) 2315-2323.
- 679 [54] B. Li, S. Kuriyama, M. Moreno, R. Mayor, The posteriorizing gene Gbx2 is a direct target of Wnt signalling
680 and the earliest factor in neural crest induction, *Development*, 136 (2009) 3267-3278.
- 681 [55] T. Zhao, Q. Gan, A. Stokes, R.N. Lassiter, Y. Wang, J. Chan, J.X. Han, D.E. Pleasure, J.A. Epstein, C.J. Zhou,
682 beta-catenin regulates Pax3 and Cdx2 for caudal neural tube closure and elongation, *Development*, (2013).
- 683 [56] S. Takada, K.L. Stark, M.J. Shea, G. Vassileva, J.A. McMahon, A.P. McMahon, Wnt-3a regulates somite and
684 tailbud formation in the mouse embryo, *Genes Dev*, 8 (1994) 174-189.
- 685 [57] K. Mizugishi, M. Hatayama, T. Tohmonda, M. Ogawa, T. Inoue, K. Mikoshiba, J. Aruga, Myogenic repressor
686 I-mfa interferes with the function of Zic family proteins, *Biochem Biophys Res Commun*, 320 (2004) 233-240.
- 687 [58] R. Houtmeyers, J. Souopgui, S. Tejpar, R. Arkell, The ZIC gene family encodes multi-functional proteins
688 essential for patterning and morphogenesis, *Cell Mol Life Sci*, 70 (2013) 3791-3811.
- 689 [59] W.J. Gehring, Y.Q. Qian, M. Billeter, K. Furukubo-Tokunaga, A.F. Schier, D. Resendez-Perez, M. Affolter, G.
690 Otting, K. Wuthrich, Homeodomain-DNA recognition, *Cell*, 78 (1994) 211-223.

- 691 [60] D. Lohnes, The Cdx1 homeodomain protein: an integrator of posterior signaling in the mouse, *Bioessays*,
692 25 (2003) 971-980.
- 693 [61] K.S. Zaret, J.S. Carroll, Pioneer transcription factors: establishing competence for gene expression, *Genes*
694 *Dev*, 25 (2011) 2227-2241.
- 695 [62] M.P. Verzi, H. Shin, A.K. San Roman, X.S. Liu, R.A. Shivdasani, Intestinal master transcription factor CDX2
696 controls chromatin access for partner transcription factor binding, *Mol Cell Biol*, 33 (2013) 281-292.
- 697 [63] B.G. Hoffman, G. Robertson, B. Zavaglia, M. Beach, R. Cullum, S. Lee, G. Soukhatcheva, L. Li, E.D. Wederell,
698 N. Thiessen, M. Bilenky, T. Cezard, A. Tam, B. Kamoh, I. Birol, D. Dai, Y. Zhao, M. Hirst, C.B. Verchere, C.D.
699 Helgason, M.A. Marra, S.J. Jones, P.A. Hoodless, Locus co-occupancy, nucleosome positioning, and H3K4me1
700 regulate the functionality of FOXA2-, HNF4A-, and PDX1-bound loci in islets and liver, *Genome Res*, 20 (2010)
701 1037-1051.
- 702 [64] K. Ohneda, R.G. Mirmira, J. Wang, J.D. Johnson, M.S. German, The homeodomain of PDX-1 mediates
703 multiple protein-protein interactions in the formation of a transcriptional activation complex on the insulin
704 promoter, *Mol Cell Biol*, 20 (2000) 900-911.
- 705 [65] Y. Litingtung, C. Chiang, Control of Shh activity and signaling in the neural tube, *Developmental dynamics* :
706 an official publication of the American Association of Anatomists, 219 (2000) 143-154.
- 707 [66] C. Chiang, Y. Litingtung, E. Lee, K.E. Young, J.L. Corden, H. Westphal, P.A. Beachy, Cyclopia and defective
708 axial patterning in mice lacking Sonic hedgehog gene function, *Nature*, 383 (1996) 407-413.
- 709 [67] K.A. Peterson, Y. Nishi, W. Ma, A. Vedenko, L. Shokri, X. Zhang, M. McFarlane, J.M. Baizabal, J.P. Junker, A.
710 van Oudenaarden, T. Mikkelsen, B.E. Bernstein, T.L. Bailey, M.L. Bulyk, W.H. Wong, A.P. McMahon, Neural-
711 specific Sox2 input and differential Gli-binding affinity provide context and positional information in Shh-
712 directed neural patterning, *Genes & development*, 26 (2012) 2802-2816.
- 713 [68] A. Marson, S.S. Levine, M.F. Cole, G.M. Frampton, T. Brambrink, S. Johnstone, M.G. Guenther, W.K.
714 Johnston, M. Wernig, J. Newman, J.M. Calabrese, L.M. Dennis, T.L. Volkert, S. Gupta, J. Love, N. Hannett, P.A.
715 Sharp, D.P. Bartel, R. Jaenisch, R.A. Young, Connecting microRNA genes to the core transcriptional regulatory
716 circuitry of embryonic stem cells, *Cell*, 134 (2008) 521-533.
- 717 [69] C.I. Wu, J.A. Hoffman, B.R. Shy, E.M. Ford, E. Fuchs, H. Nguyen, B.J. Merrill, Function of Wnt/beta-catenin
718 in counteracting Tcf3 repression through the Tcf3-beta-catenin interaction, *Development*, 139 (2012) 2118-
719 2129.
- 720 [70] F. Gofflot, M. Hall, G.M. Morriss-Kay, Genetic patterning of the developing mouse tail at the time of
721 posterior neuropore closure, *Developmental dynamics* : an official publication of the American Association of
722 Anatomists, 210 (1997) 431-445.
- 723 [71] T. Inoue, M. Ota, K. Mikoshiba, J. Aruga, Zic2 and Zic3 synergistically control neurulation and segmentation
724 of paraxial mesoderm in mouse embryo, *Developmental biology*, 306 (2007) 669-684.
- 725 [72] T. Inoue, M. Ota, M. Ogawa, K. Mikoshiba, J. Aruga, Zic1 and Zic3 regulate medial forebrain development
726 through expansion of neuronal progenitors, *The Journal of neuroscience* : the official journal of the Society for
727 Neuroscience, 27 (2007) 5461-5473.
- 728 [73] J. Aruga, T. Inoue, J. Hoshino, K. Mikoshiba, Zic2 controls cerebellar development in cooperation with Zic1,
729 *J Neurosci*, 22 (2002) 218-225.
- 730 [74] T. Inoue, M. Ogawa, K. Mikoshiba, J. Aruga, Zic deficiency in the cortical marginal zone and meninges
731 results in cortical lamination defects resembling those in type II lissencephaly, *J Neurosci*, 28 (2008) 4712-4725.
- 732 [75] C.P. Chang, K. Stankunas, C. Shang, S.C. Kao, K.Y. Twu, M.L. Cleary, Pbx1 functions in distinct regulatory
733 networks to pattern the great arteries and cardiac outflow tract, *Development*, 135 (2008) 3577-3586.

734
735
736
737
738

739 **FIGURE LEGENDS**

740

741 **FIGURE 1:** Partially overlapping Cdx and *Pax3* expression domains indicate that Cdx proteins are
 742 necessary but not sufficient to establish the *Pax3* expression domain in the caudal neuroectoderm.

743 (A) Immunofluorescence analysis of Cdx2 and *Pax3* distribution in tailbud sections of a 25-somite
 744 stage mouse embryo (e9.5). The dashed red lines in the left panel indicate the AP level at which the
 745 sections shown on the right were made (A', A'', A'''). The dotted white lines in the right panel delimit
 746 the posterior neural plate (PNP) and the neural tube (NT) structures. Note that Cdx2 is broadly
 747 expressed in the tailbud including the whole PNP (A') and, more rostrally, in the entire NT (A'', A''')
 748 while *Pax3* domain is limited to the lateral borders of the PNP (A') and to the dorsal part of the NT
 749 (A'', A'''). (B) Schematic drawing of two putative mechanisms to explain the induction and dorsal
 750 restriction of *Pax3* neural expression (pink) via Cdx proteins (green). (B') *Pax3* expression at the lateral
 751 borders of the PNP might be established by collaboration between Cdx proteins and a positive input
 752 from a neural-specific protein with more-or-less restricted expression: i.e. a Cdx cofactor expressed in
 753 the PNP (yellow) or at the lateral borders of the PNP (purple) [Mechanism 1]. Restriction of *Pax3*
 754 expression at the PNP border may also be achieved by integration of the positive Cdx input with the
 755 negative input from a repressor expressed in the medial PNP (red) [Mechanism 2]. (B'') At more
 756 rostral levels, where Cdx expression is restricted to the NT, the Cdx input might be integrated with the
 757 positive input from a dorsally restricted Cdx cofactor (blue) [Mechanism 1] and/or the negative input
 758 from a ventrally expressed repressor (red) [Mechanism 2].

759

760 **FIGURE 2:** The *Zic2* transcription factor regulates *Pax3* expression.

761 (A-J) Overlapping spatiotemporal *Zic2* and *Pax3* expression patterns are consistent with a role for *Zic2*
 762 in regulating *Pax3* expression. (A-B) Lateral view of 20-somite stage embryos (~e9.0) with anterior to
 763 the left showing *Zic2* (A) and *Pax3* (B) expression domains assessed by whole-mount *in situ*
 764 hybridisation. (C-J) Comparison of *Zic2* and *Pax3* expression domains in the caudal end of 24-somite
 765 stage embryos (~e9.5). The dotted lines in the lateral views shown in C-D indicate the level at which
 766 the transverse sections shown in G-J were cut. The red brackets in E-F designate the length of the
 767 caudal tip of the tailbud region (dorsal view) that is devoid of *Zic2* and *Pax3* gene expression. Note
 768 that, compared to *Pax3*, the *Zic2* expression domain in the open PNP extends more posteriorly (C-H).
 769 Also note the extensive overlap in *Pax3* and *Zic2* expression in the dorsal NT (C-D; red brackets in I-
 770 J). *Pax3* and *Zic2* expression patterns do not overlap in the developing somites. The presomitic
 771 mesoderm (C, D) and somites (I, J) are denoted by asterisks. (K) Analyses of endogenous *Pax3*
 772 expression in N2a cells transfected with increasing amounts of a $HAZic2$ -IRES-GFP expression vector.
 773 GFP-positive N2a cells were recovered by FACS and exogenous $HAZic2$ as well as endogenous *Pax3*
 774 expression were analyzed by western blot and RT-PCR, respectively. Note that increasing levels of
 775 $HAZic2$ (left panel) result in a dose-dependent increase of endogenous *Pax3* expression but not *Gapdh*
 776 used as control (right panel).

777

778 **FIGURE 3:** *Zic2* activates and directly binds the *Pax3* neural crest enhancer NCE2.

779 (A) Co-transfection assays in N2a cells using luciferase reporter constructs driven by the *Pax3*NCE2
 780 region plus the *Pax3* 150bp minimal promoter (*Pax3*NCE2-min-Luc) or only driven by the *Pax3* 150bp

781 minimal promoter (*Pax3*min-Luc) as well as a *HAZic2* expression vector. The luciferase quantification
 782 results are expressed as fold activation compared to each reporter vector alone. n=5 independent
 783 experiments performed in triplicate; one-way ANOVA: P<0.0001; Tukey's post test: n.s. P>0.05; *
 784 P<0.05; ***: P<0.001. Error bars indicate s.e.m. Note that increasing *Zic2* expression significantly
 785 increases the activation of the *Pax3*NCE2 reporter but not the *Pax3*min reporter. (B) Identification of
 786 *Zic* binding sites in the *Pax3*NCE2 by electrophoretic mobility shift assay (EMSA). Eight overlapping
 787 double-stranded oligonucleotide probes (represented as numbers 1 to 8 in boxes at the top of each
 788 panel) were used to scan the whole NCE2 for *Zic* binding sites (*Zic*BS). A probe bearing a consensus
 789 Gli/*Zic*BS [41] was used as a positive control for *Zic* binding. All *in vitro* binding reactions were
 790 performed in parallel under identical conditions and each probe was either not incubated (-), or
 791 incubated with nuclear extracts from Mock- (transfected without DNA) or *HAZic2*-transfected Cos7
 792 cells. Note that, similarly to the shifted band observed with the positive control (*Zic*BS), a specific
 793 shifted band is observed for radiolabelled probe #3 (red box) when incubated with *HAZic2* nuclear
 794 extracts. (C) Chromatin immunoprecipitation assays in N2a cells showing the occupancy of *Pax3*NCE2
 795 by both *FLAGCdx1* and *HAZic2*. Anti-FLAG-, anti-HA- or normal rabbit IgG-immunoprecipitated
 796 chromatin extracts from *FLAGCdx1*- and *HAZic2*- transfected N2a cells were purified and amplified by
 797 PCR using primers flanking the *Pax3*NCE2 region. Amplification products, resolved on a 2% agarose
 798 gel, were of the expected size (246bp) and sequence-confirmed. Lanes 1, 2 and 3 represent PCR
 799 amplifications of serial dilutions of DNA. Note that *Pax3*NCE2 is amplified from chromatin samples
 800 immunoprecipitated with anti-FLAG (*Cdx1*) and anti-HA (*Zic2*), but not with the non-specific IgG.

801

802 **FIGURE 4:** *Zic2* and *Cdx1* directly interact via their respective DNA binding domain.

803 (A) Co-immunoprecipitation assay using whole cell lysates from Cos7 cells transfected with *FLAGCdx1*
 804 and/or *HAZic2* expression vectors. Total lysates were immunoprecipitated with anti-FLAG antibody and
 805 analyzed by immunoblotting using an anti-HA antibody (top panel). Expression of *Cdx1* was assessed
 806 by reprobing the blot with an anti-FLAG antibody (middle panel). Inputs represent 5% of the total
 807 lysate used for immunoprecipitation. (B-C) Mapping of *Cdx1* and *Zic2* interacting domains via GST
 808 pull-down assays. Inputs represent 15% of the total *in vitro*-translated proteins used for pull-downs. (B)
 809 Western blot using an anti-FLAG antibody showing that human *FLAGZIC2* specifically interacts with
 810 both full-length *Cdx1* (GST-*Cdx1*) and *Cdx1* homeodomain (GST-*Cdx1*Homeo) but not with the *Cdx1*
 811 N-terminal region (GST-*Cdx1*Nterm). (C) The Zinc finger domain of *ZIC2* is essential for the
 812 interaction with the *Cdx1* homeodomain. Different *FLAGZIC2* deletion constructs were used to identify
 813 *ZIC2* regions that interact with the *Cdx1* homeodomain. Note that deletion of the five Cys2His2-type
 814 zinc fingers (construct 1-255) specifically abolishes interaction with the *Cdx1* homeodomain. (D)
 815 Schematic representation of *ZIC2* and its deletion constructs (adapted from [34] and [58]) and their
 816 interaction with *Cdx1*. (E) Characterization of the *Zic* binding site (*Zic*BS) contained in NCE2 and
 817 evaluation of the interaction of *Zic2* and *Cdx1* in the presence of their target DNA by EMSA. Results
 818 with a probe containing the new *Zic*BS (NCE2 scanning probe 3) are shown in E' while results with
 819 probes containing the previously described *Cdx*BS1 (NCE2 scanning probe 5) or *Cdx*BS3 (NCE2
 820 scanning probe 2) are shown in E'' and E''', respectively. All *in vitro* binding reactions were
 821 performed in parallel under identical conditions. Binding of *HAZic2* and *FLAGCdx1* as well as anti-HA
 822 supershift (SS) and non-specific bindings (NS) are indicated by arrows. Brackets and asterisks denote

823 the presence of higher molecular weight bands when $_{HA}Zic2$ - and $_{FLAG}Cdx1$ -overexpressing nuclear
 824 extracts are used in combination. Note that specificity of *Zic2* binding to the new *ZicBS* was evaluated
 825 by pre-incubation of nuclear extracts from $_{HA}Zic2$ - or mock-transfected Cos7 cells with a 100-fold
 826 molar excess of non-radiolabeled wild type (wt) or mutated (mt) probes. Sequences of the *ZicBS* as
 827 well as its mutated version used to assess *Zic2* binding specificity by EMSA are at the bottom of E';
 828 point mutations are denoted in green.

829

830 **FIGURE 5:** Cdx1 and *Zic2* functionally interact and synergize with the SoxB1 family member Sox2
 831 in the transactivation of *Pax3*NCE2.

832 (A) Cdx1 and *Zic2* cooperatively transactivate *Pax3*NCE2 in N2a cells and Cdx binding sites (CdxBS)
 833 are essential for this functional interaction. A wild type (wt) *Pax3*NCE2-luciferase reporter (1) or
 834 mutant versions bearing mutations in the three CdxBS (2), the *ZicBS* (3) or a combination of these
 835 mutations (4) were evaluated for Cdx1 and *Zic2* transactivation in N2a cells. Note that $_{FLAG}Cdx1$ and
 836 $_{HA}Zic2$ co-transfection results in a transactivation of the wt *Pax3*NCE2-luc reporter stronger than
 837 simple addition of each single transfections, and that mutation of CdxBS and/or *ZicBS* abrogates this
 838 cooperative effect. In contrast, the transactivating effect of *Zic2* is not affected by mutation of CdxBS
 839 and/or *ZicBS*. (B) Schematic representation of the *Pax3* genomic locus showing the relative position of
 840 *Pax3* regulatory regions. The 5' regulatory region (represented as a blue box) is named NCE and is
 841 subdivided in two CRMs called NCE1 and NCE2 [28]. The intron-4 regulatory region (red box)
 842 contains the CNE3 and CNE1 modules [30]. Black boxes represent exons. (B') Magnification view of
 843 *Pax3*NCE2 DNA sequence showing the location of the *ZicBS* as well as the three functional CdxBS (in
 844 boxes) and in relation to a putative SoxBS (MatInspector analyses) as well as the previously described
 845 *Brn1/2* [31] and *Tead* binding sites [28] (underlined). (C) Sox2 strongly activates *Pax3*NCE2 in N2a
 846 cells, but cannot activate this CRM in undifferentiated P19 cells. N2a and P19 cells were equally
 847 transfected with the *Pax3*NCE2-luc reporter alone or with increasing amounts of the Sox2 expression
 848 vector. (D) Cdx1, *Zic2* and Sox2 act synergistically in the transactivation of *Pax3*NCE2 in N2a cells.
 849 Cells were transiently transfected with the *Pax3*NCE2-luc reporter alone or co-transfected with
 850 $_{FLAG}Cdx1$, $_{HA}Zic2$ or $_{Myc}Sox2$ expression vector alone or in combination. In A, C and D, results are
 851 expressed as fold activation compared to the relevant reporter vector alone. n=6-10 independent
 852 experiments performed in triplicate; one-way ANOVA: $P < 0.0001$; Tukey's post test: n.s. $P > 0.05$; *
 853 $P < 0.05$; ***: $P < 0.001$. Error bars indicate s.e.m.

854

855 **FIGURE 6:** *Zic2* and *Zic5* are potential intermediates in the Shh-induced repression of *Pax3*
 856 expression.

857 (A-O) Comparison of *Pax3* and *Zic2* expression domains (assessed by whole-mount *in situ*
 858 hybridisation), with *Nkx6.1* distribution (assessed by whole-mount immunofluorescence) in serial
 859 vibratome sections of the posterior end of 24-somite (e9.5) stage-matched embryos (caudal to rostral
 860 direction). Note that restricted *Pax3* expression in the open PNP (A) and recently closed NT (B) is
 861 established before the onset of *Nkx6.1* expression in the ventral NT (red arrow in M). Also note that the
 862 onset of *Zic2* repression in the ventral NT (red arrow in H) correlates with the presence of *Nkx6.1* in
 863 this region (red arrow in M). Going forward in the posterior to anterior direction, *Zic2* and *Nkx6.1*
 864 expression domains are complementary along the dorsal-ventral axis [i.e.: ~90% (H) vs ~10% (M);

865 ~60% (I) vs ~40% (N); ~40% (J) vs ~60% (O)]. In contrast, *Pax3* and *Nkx6.1* expression domains only
 866 become complementary at the most rostral levels [~40% (E) vs ~60% (O)]. (*P-Q*) Analysis of *Pax3*,
 867 *Zic2* and *Zic5* gene expression in Shh-treated N2a cells via semi-quantitative RT-PCR. Results shown
 868 are representative of at least two independent experiments. (*P*) The *Zic2-Zic5* gene pair is, like *Pax3*,
 869 expressed in N2a cells and negatively regulated by Shh in a dose-dependent manner. Prior to RT-PCR
 870 analysis, cells were cultured in absence or presence of increasing doses of Shh over a fixed 24-hour
 871 period of time. (*Q*) *Zic2* is an intermediary in the mechanism of *Pax3* repression by Shh. Prior to RT-
 872 PCR analysis, cells were transfected with _{HA}*Zic2* or empty IRES-GFP expression vector and then
 873 cultured for 24h in Ctl or Shh-enriched medium. Note that overexpression of *Zic2* prevents the Shh-
 874 induced repression of *Pax3* in FACS-recovered N2a cells.

875

876 **FIGURE 7:** Current model for the Cdx-dependent control of *Pax3* expression in the caudal
 877 neuroectoderm via the NCE2 CRM.

878 Neural-specific induction of *Pax3* expression by the previously described Wnt-Cdx circuit requires an
 879 interaction with *Zic2/5* and *Sox2*. Supplemental unknown (?) positive and/or negative inputs are
 880 required to restrict the *Pax3* expression domain to the lateral borders of the PNP. Maintenance of
 881 restricted NCE2 activity in the dorsal NT is most likely mediated by the dorsally restricted *Zic2/5*
 882 transcription factors, which act as Cdx cofactors and are the predicted immediate early targets of the
 883 Shh-*Nkx6.1* repression pathway. As elongation proceeds and the Cdx input disappears, *Pax3*
 884 expression in the NT is also later maintained by *Tead2* and *Brn1/2* transcription factors.

885

886

887 **FIGURE S1:** ZIC2 and Cdx1 can still physically interact in presence of the NCE2.

888 (A) Anti-FLAG western blot showing the expected size of *in vitro*-translated FLAG-tagged full-length
 889 (_{FLAG}ZIC2(1-532)) and truncated ZIC2 proteins (_{FLAG}ZIC2(140-532); _{FLAG}ZIC2(1-255); _{FLAG}ZIC2(1-
 890 415); _{FLAG}ZIC2(255-532)). (B) ZIC2 and Cdx1 bind to each other via their DNA binding domain. GST
 891 and GST-Cdx1 homeodomain (GST-Cdx1Homeo) fusion proteins were bound to glutathione-agarose
 892 beads and then incubated with *in vitro*-translated full-length or truncated _{FLAG}ZIC2 proteins. Presence
 893 of _{FLAG}ZIC2 in the precipitated complexes was then analysed by Western blot using an anti-FLAG
 894 antibody. Inputs represent 15% of the total *in vitro*-translated proteins used for pull-downs. Note that
 895 specific bindings are observed with _{FLAG}ZIC2(1-532), _{FLAG}ZIC2(140-532), _{FLAG}ZIC2(1-415) and
 896 _{FLAG}ZIC2(255-532) proteins but not with the truncated version _{FLAG}ZIC2 1-255 lacking the zinc finger
 897 domain. (C) Anti-FLAG immunoblot analysis of the interaction between _{FLAG}ZIC2(1-532) and GST-
 898 Cdx1Homeo in presence of the target NCE2 DNA. Note that, in comparisons to standard pull-down
 899 conditions (lanes 1-3), using EMSA buffer conditions does not affect the interaction (lanes 4-5). Note
 900 also that variations in signal intensity detected in lanes 6-7 are independent of the amount of NCE2
 901 sequences.

902

903 **FIGURE S2:** Western blot validation of the expression of Cdx1, *Zic2* and *Sox2* in N2a lysates used for
 904 luciferase reporter assays.

905 Expression vectors for _{FLAG}Cdx1, _{HA}*Zic2* as well as _{Myc}*Sox2* were transfected alone or in different
 906 combinations together with a luciferase reporter construct driven by the *Pax3NCE2* and the *Pax3*

907 minimal promoter (*Pax3NCE2*-min-Luc). Production of exogenous proteins was evaluated by western
908 blot using anti-FLAG, anti-HA as well as anti-Myc antibodies. Shown are the luciferase quantification
909 results (expressed as fold activation compared to the reporter vector alone) as well as western blot
910 validations for one representative experiment of the results displayed in Fig.5D.

911

912 **FIGURE S3:** The N2a cell line is a good model for studying the Shh-induced repression of *Pax3*
913 expression.

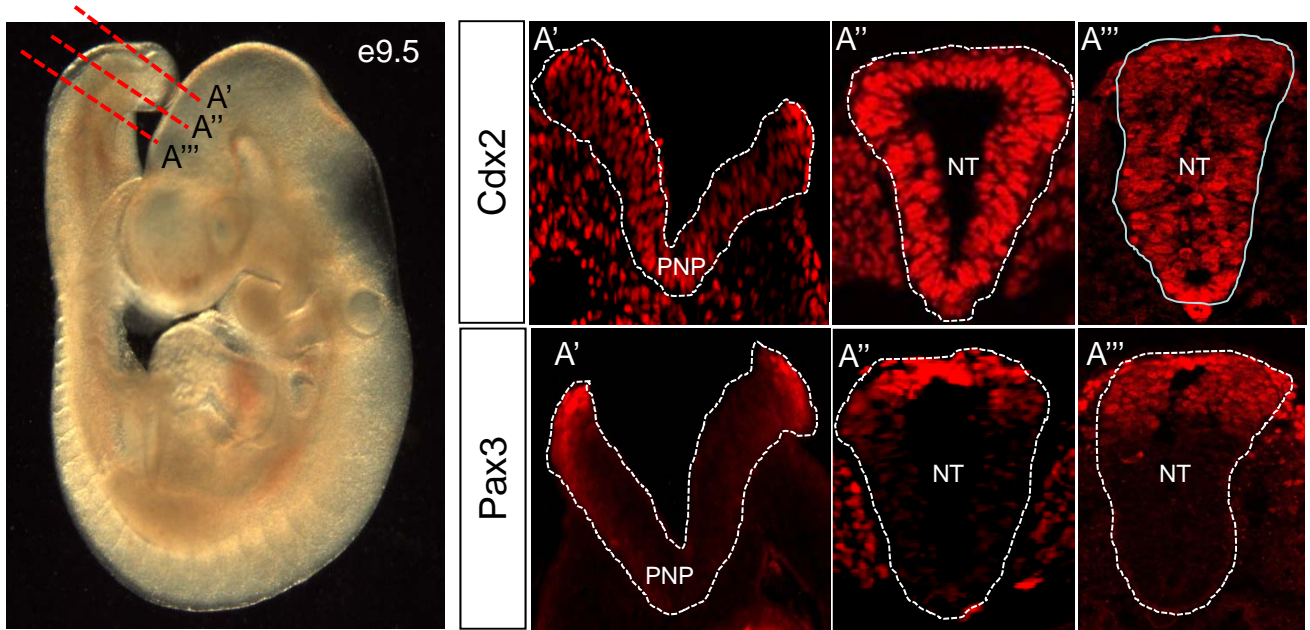
914 (A,B) RT-PCR analysis demonstrating that *Pax3* expression is indirectly repressed by Shh signaling in
915 N2a cells. Prior to RT-PCR, cells were cultured for 24h in absence or presence of Shh and/or absence
916 or presence of cyclopamine or cycloheximide (CHX). Results are representative of at least n=3
917 independent experiments. (A) *Pax3* expression is repressed by Shh in a dose-dependent manner (left
918 panel) and this repression is abrogated in presence of cyclopamine, an inhibitor of the Shh receptor
919 Smo (right panel). (B) *De novo* protein synthesis is required for the Shh-mediated repression of *Pax3*
920 expression, as shown here in presence of the translation inhibitor CHX.

921

922

A

Caudal \longrightarrow Rostral



B

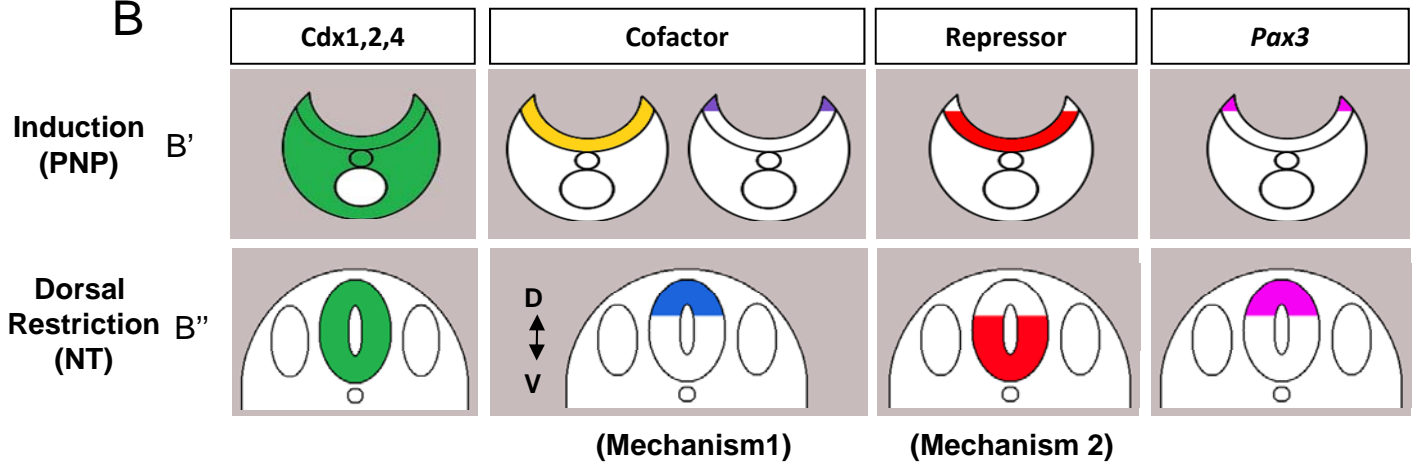
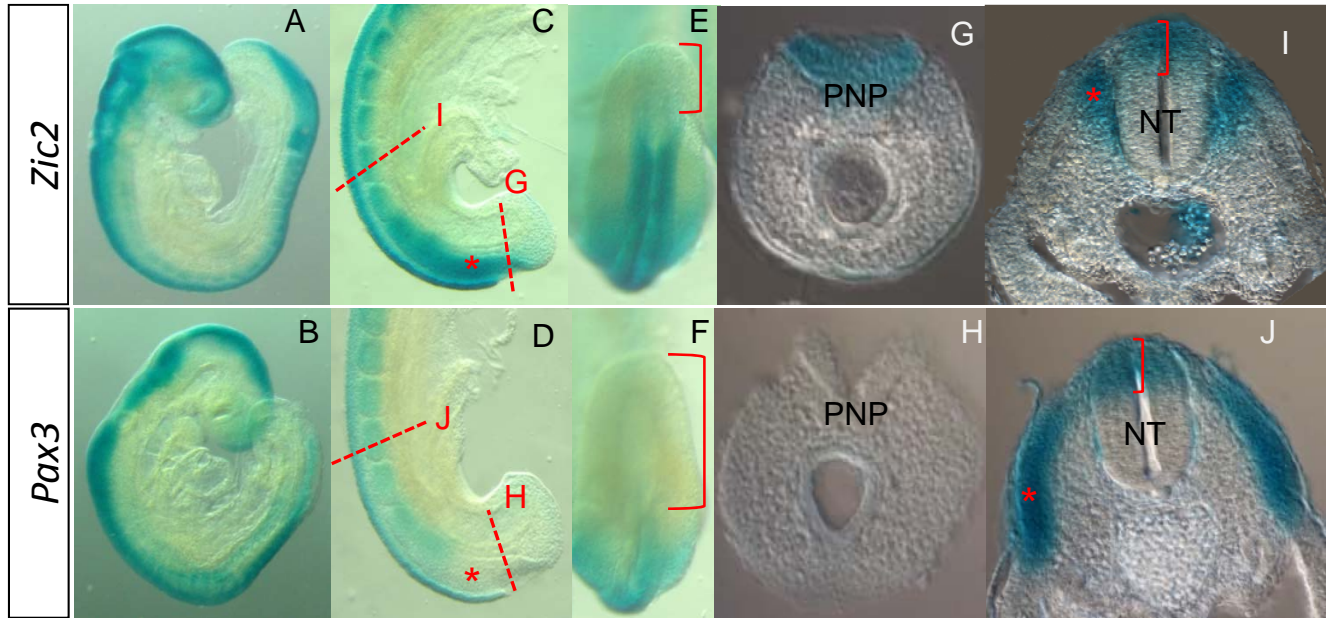


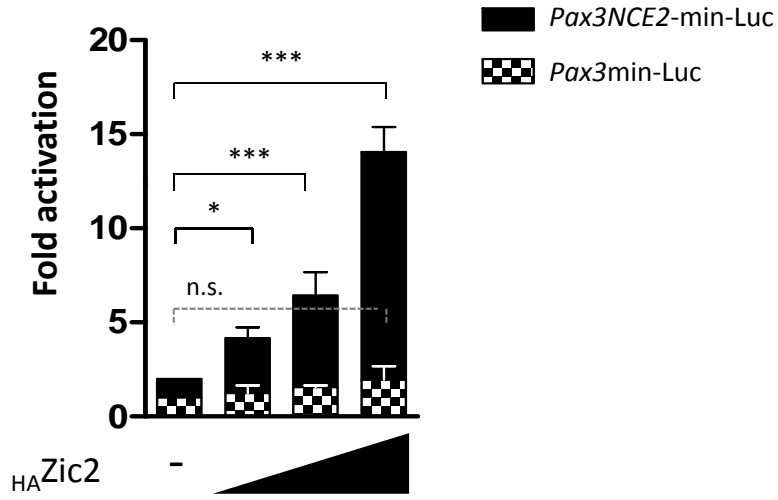
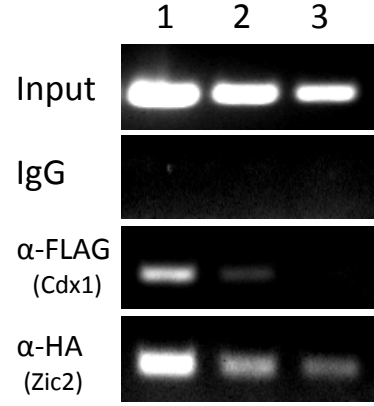
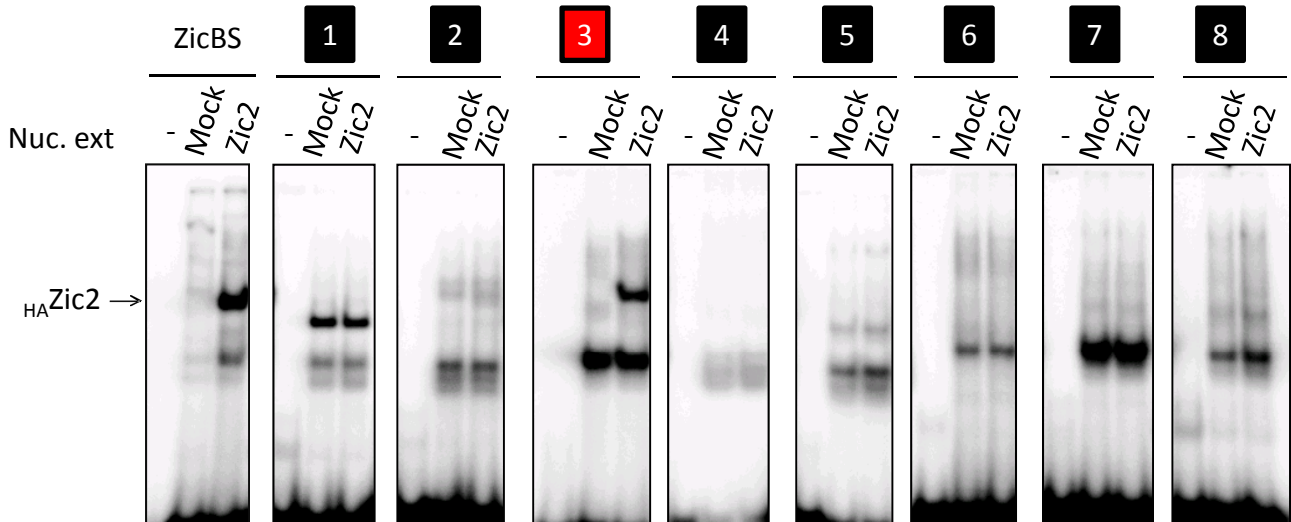
FIGURE 1



K



FIGURE 2

A**C****B****FIGURE 3**

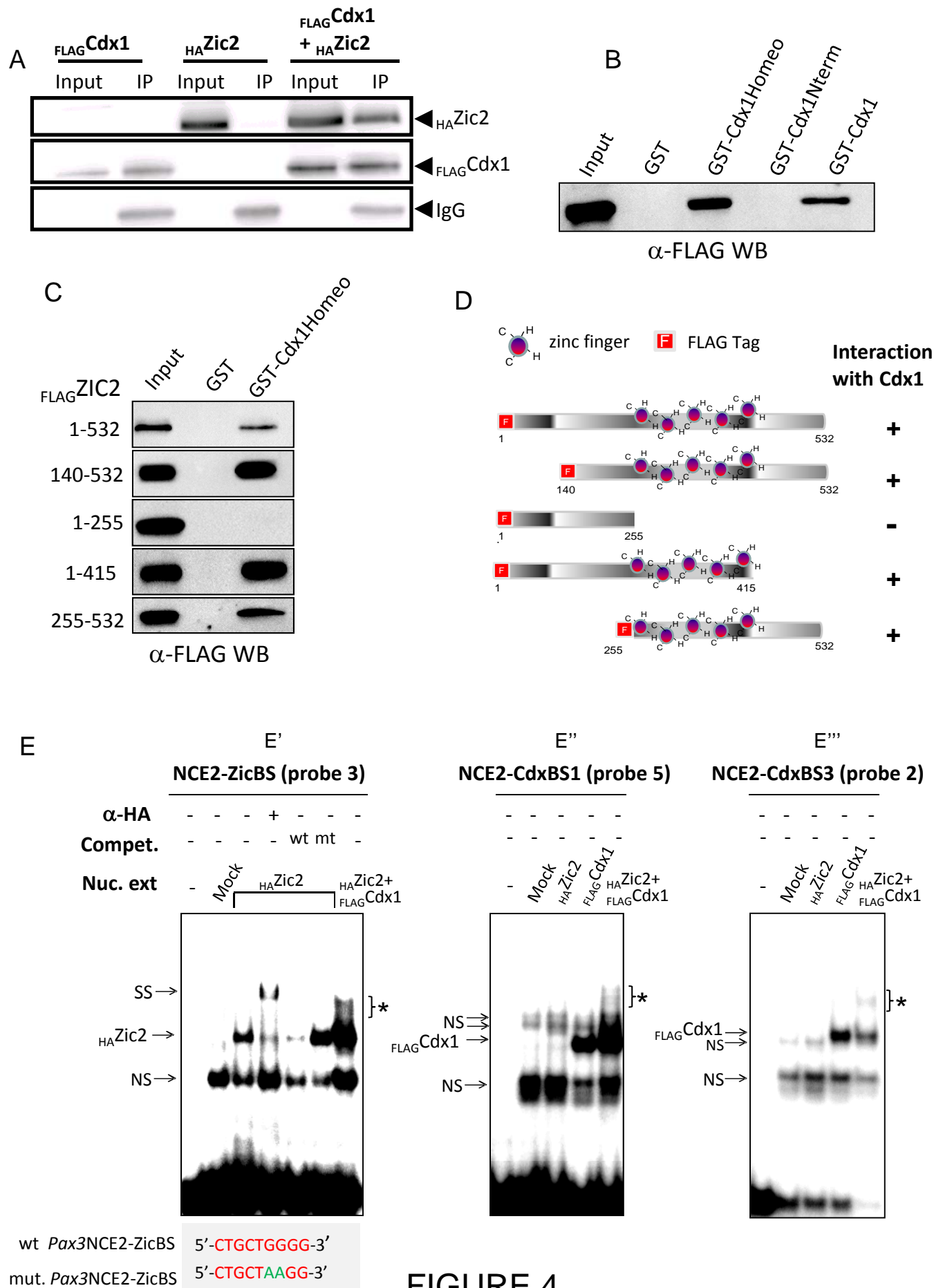


FIGURE 4

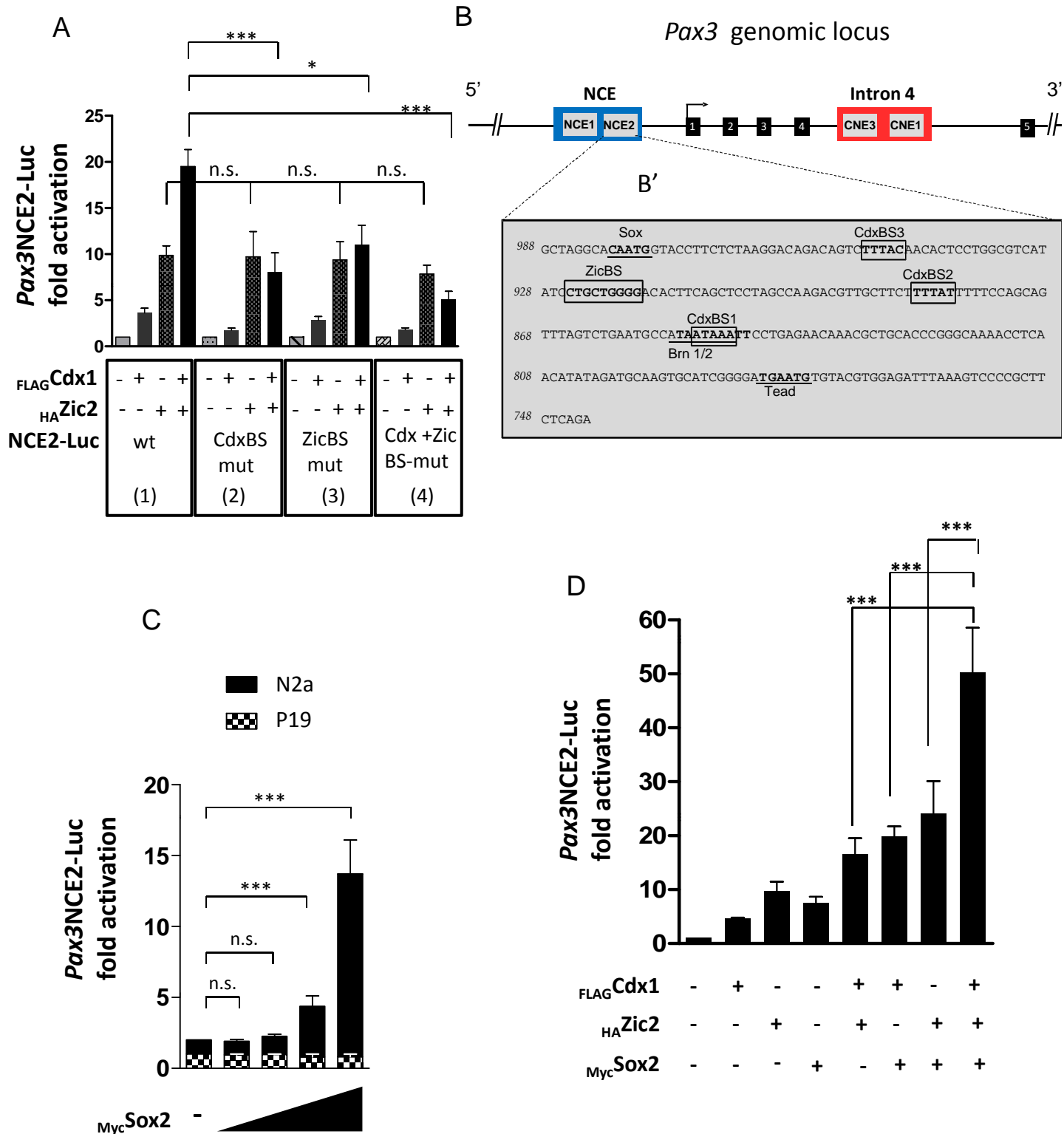


FIGURE 5

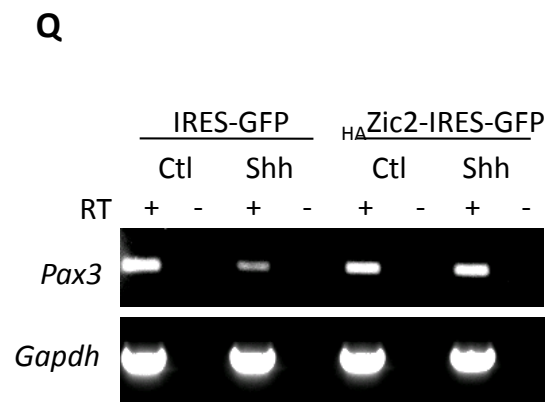
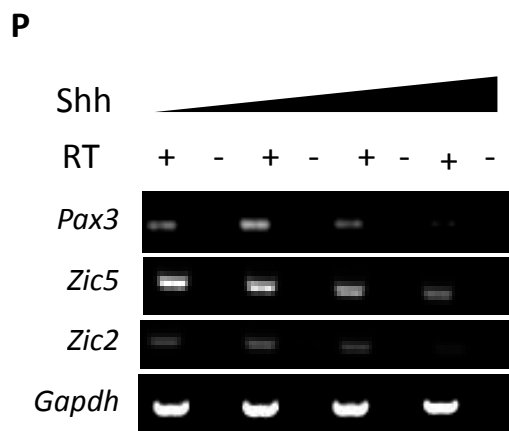
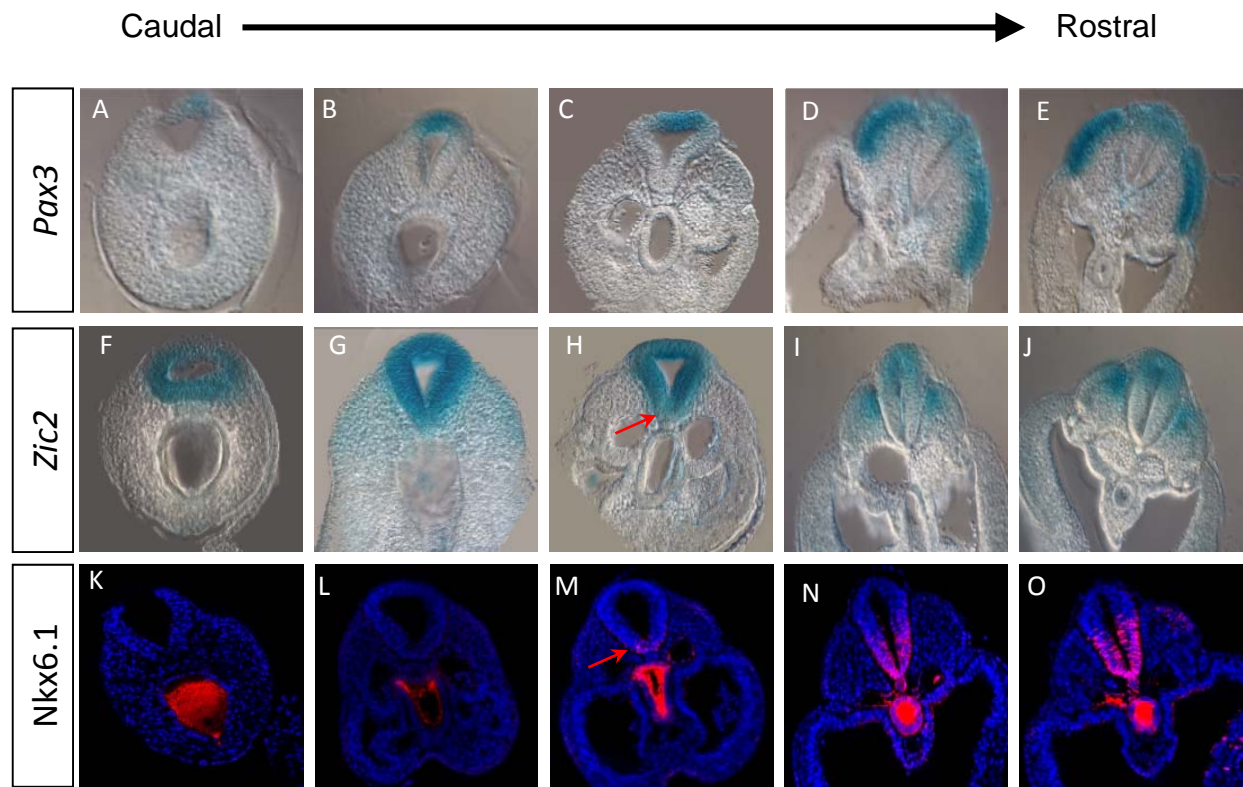


FIGURE 6

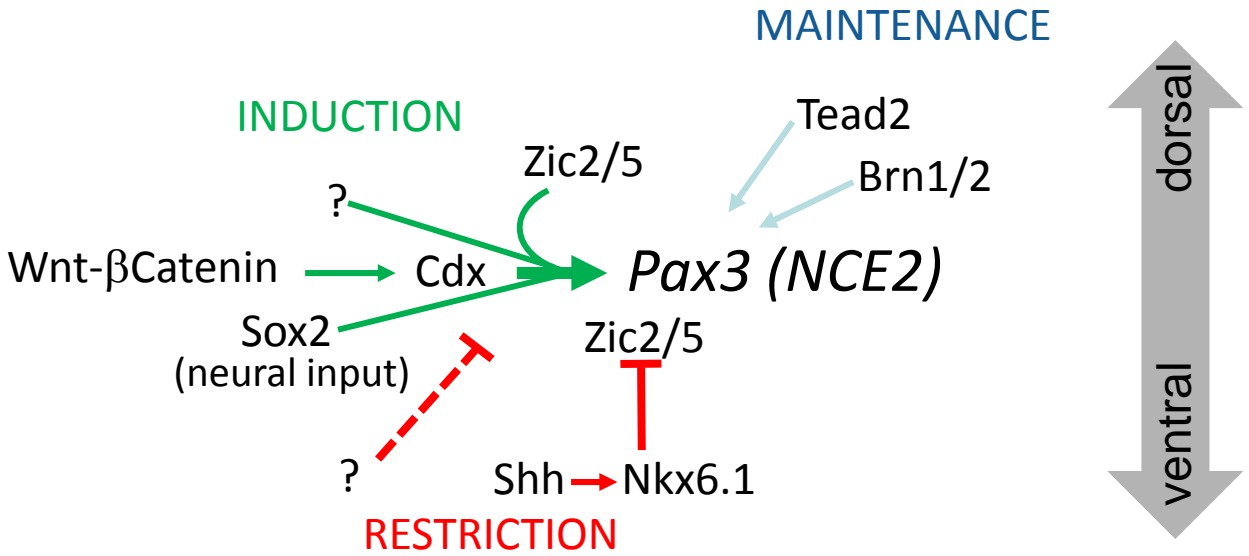
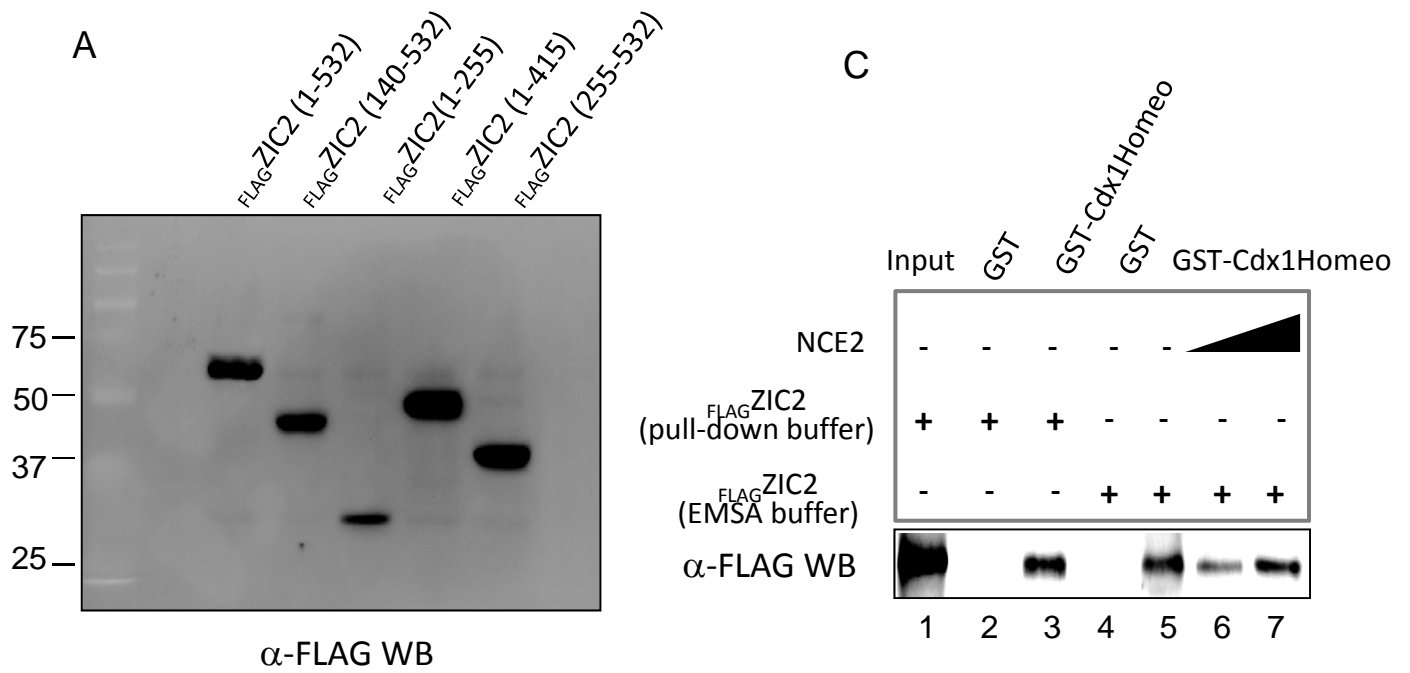


FIGURE 7



B

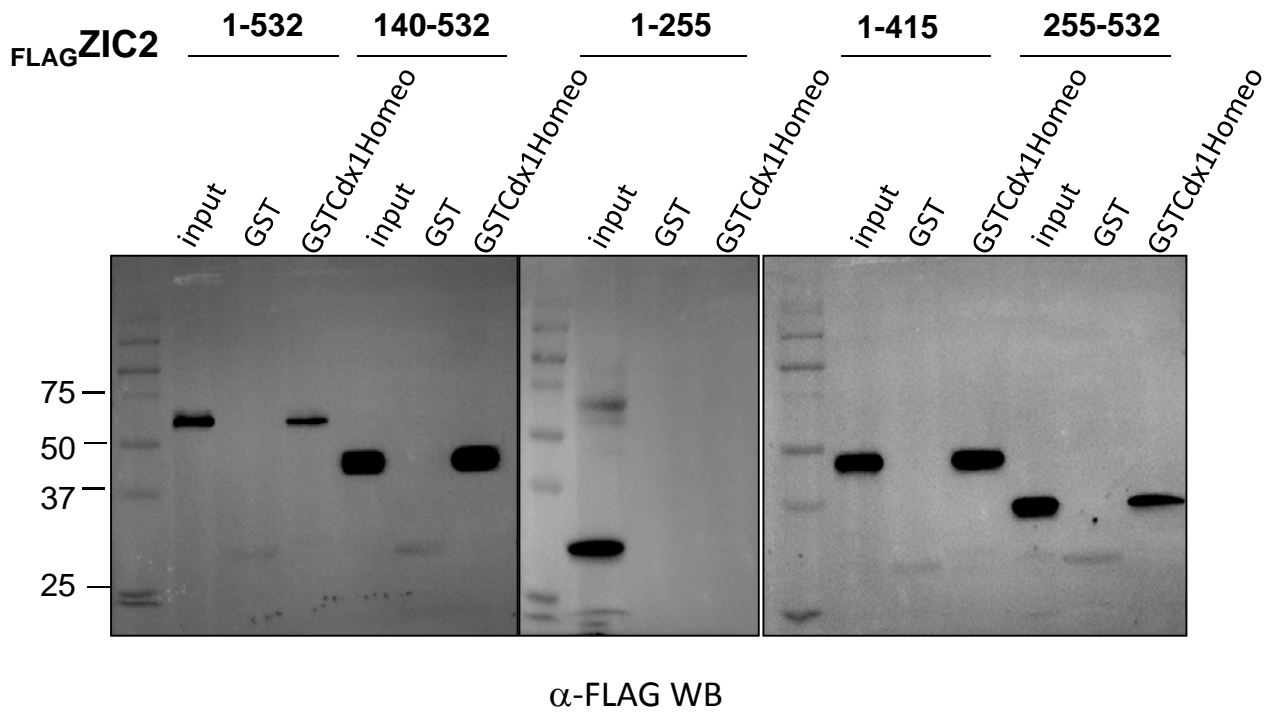


FIGURE S1

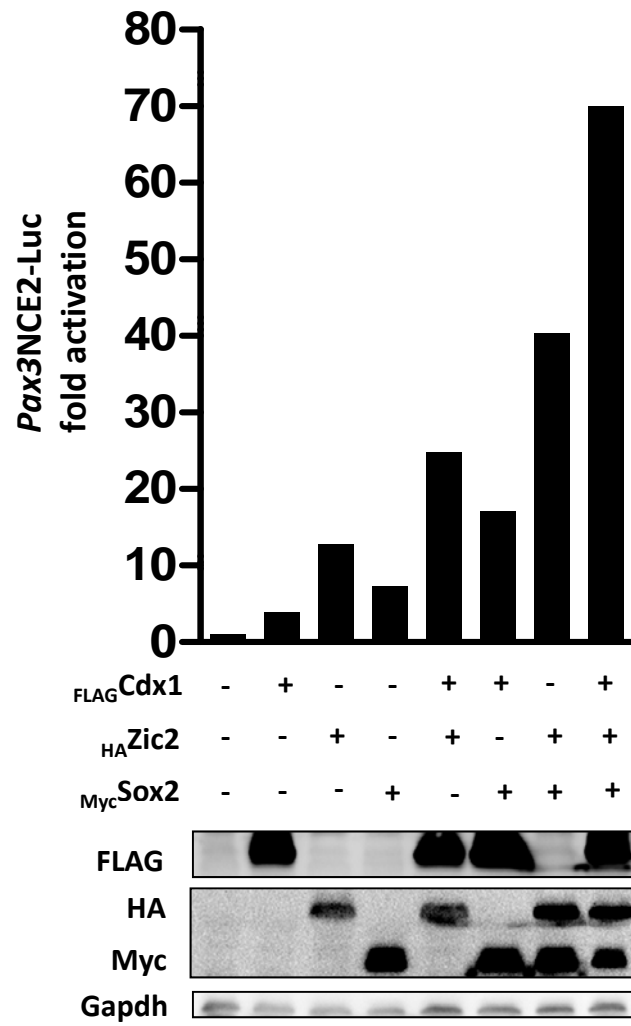


FIGURE S2

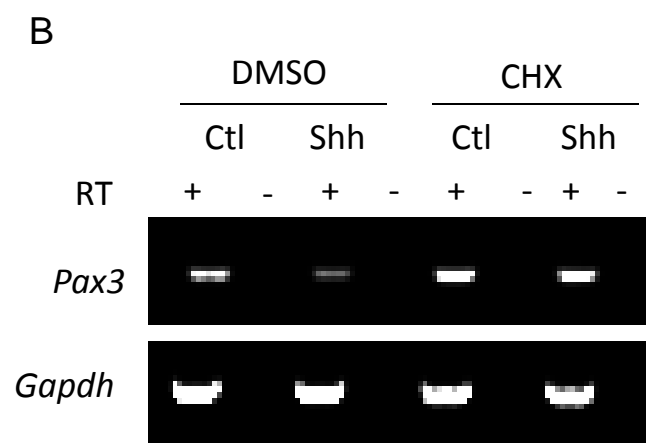
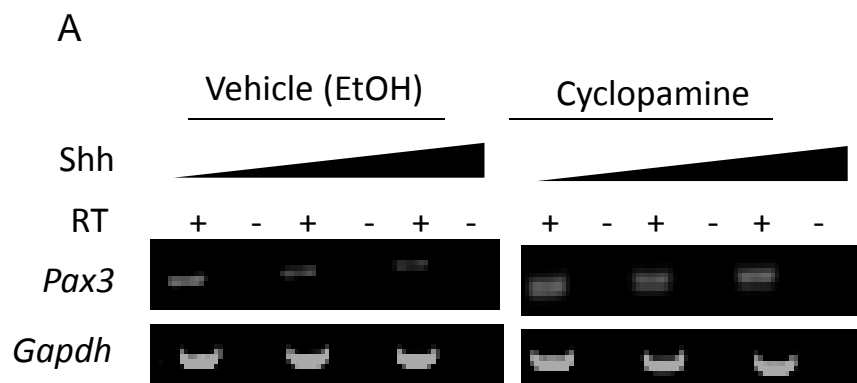


FIGURE S3